

COSMIC MAGNETIC FIELDS

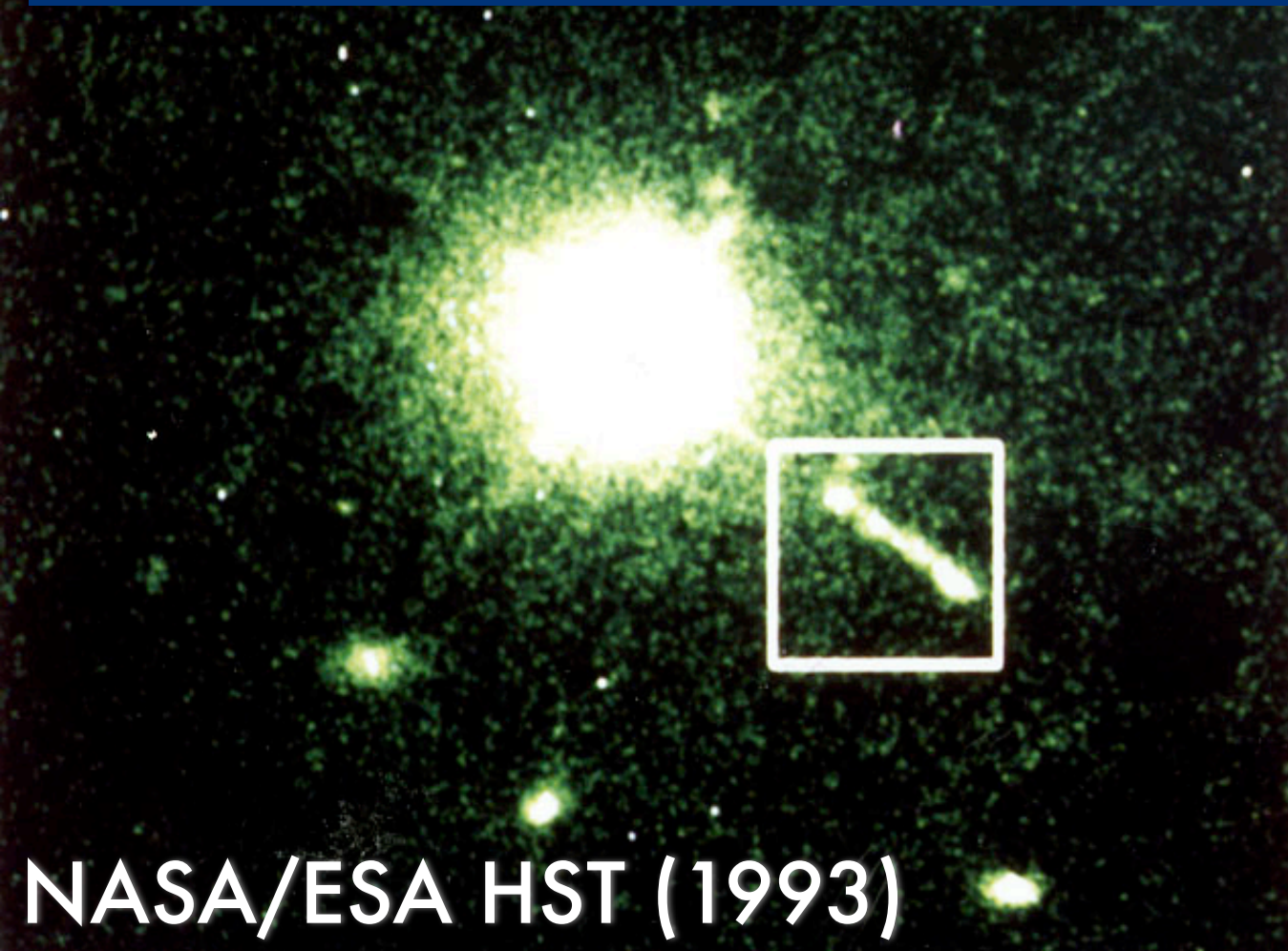
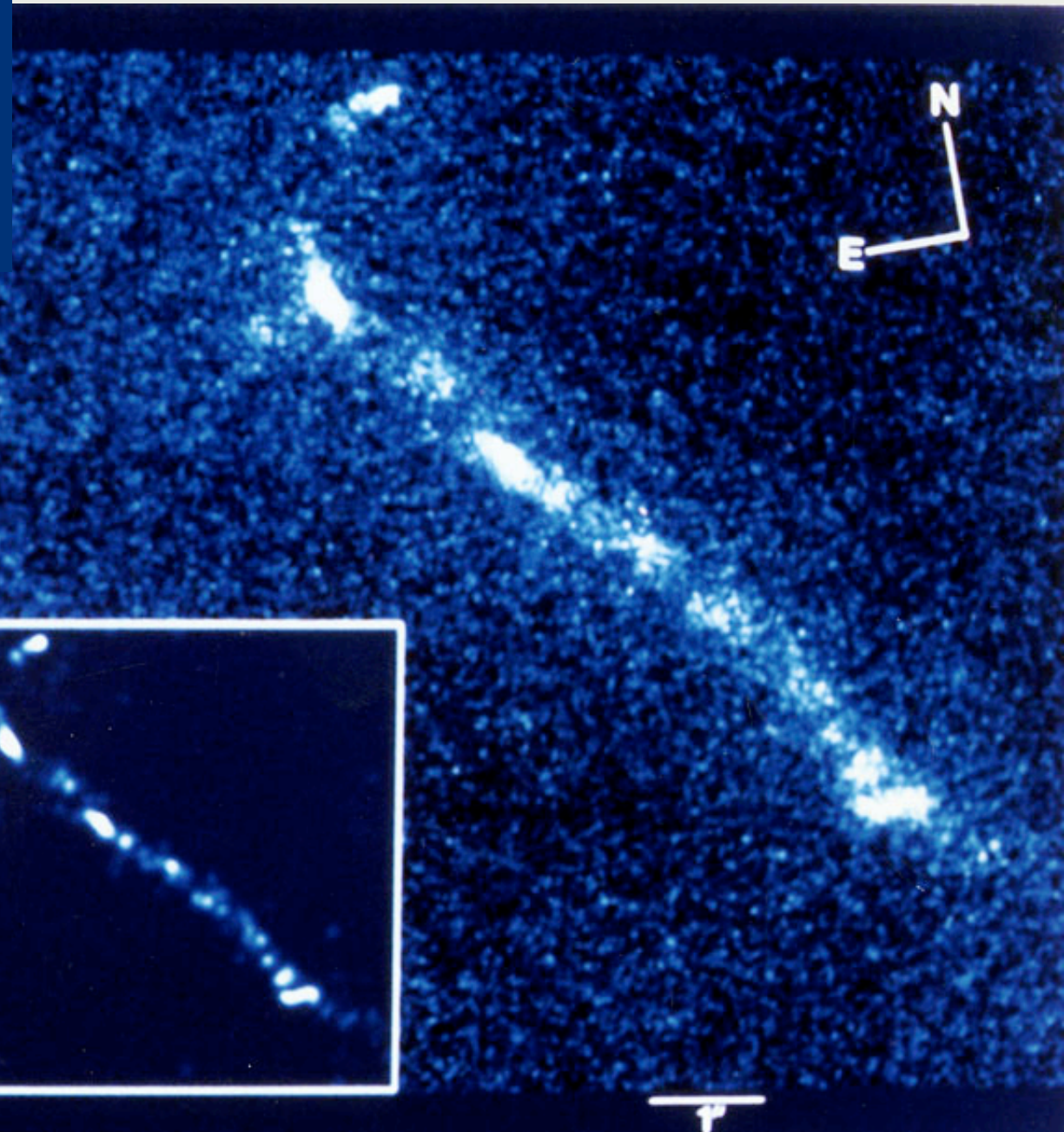
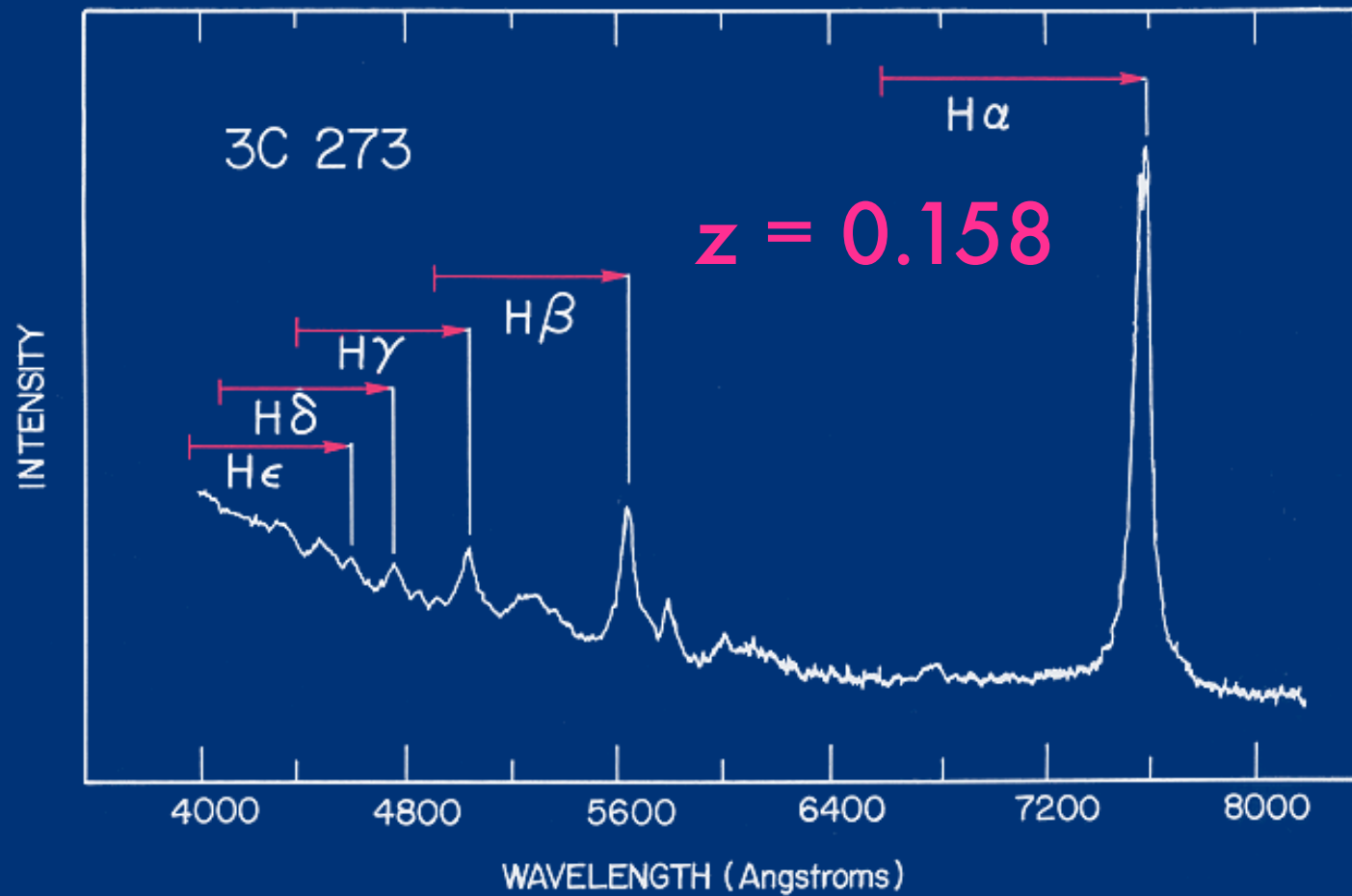
KRZYSZTOF NALEWAJKO, CAMK PAN

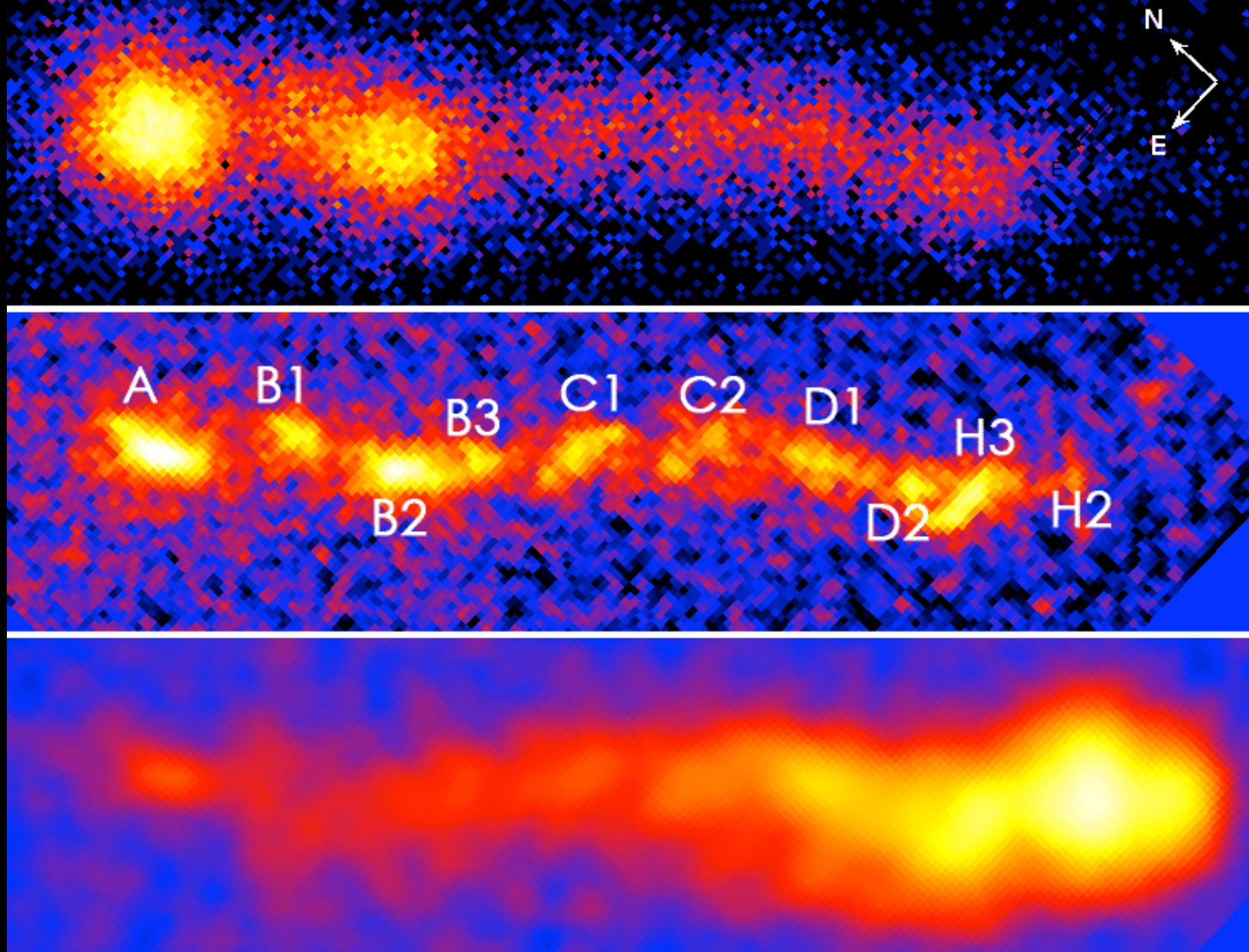
KNALEW@CAMK.EDU.PL

Jets

ACTIVE GALACTIC NUCLEI

QUASAR 3C 273





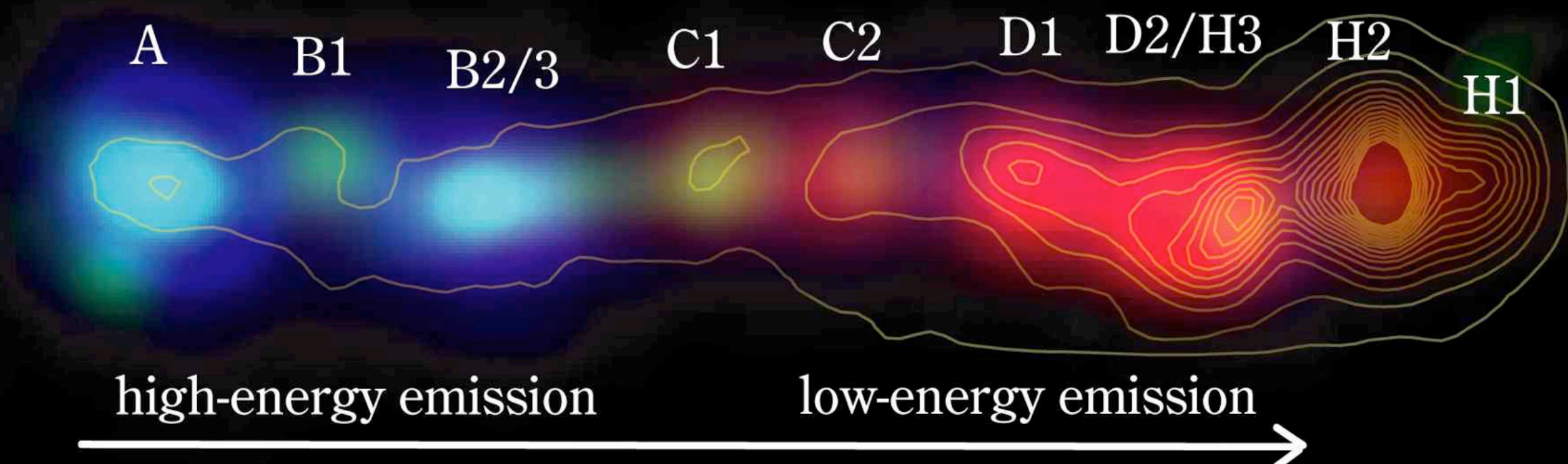
Chandra

Hubble

VLA

3C 273 jet VLA Spitzer* Hubble Chandra
 Uchiyama et al. (2006)

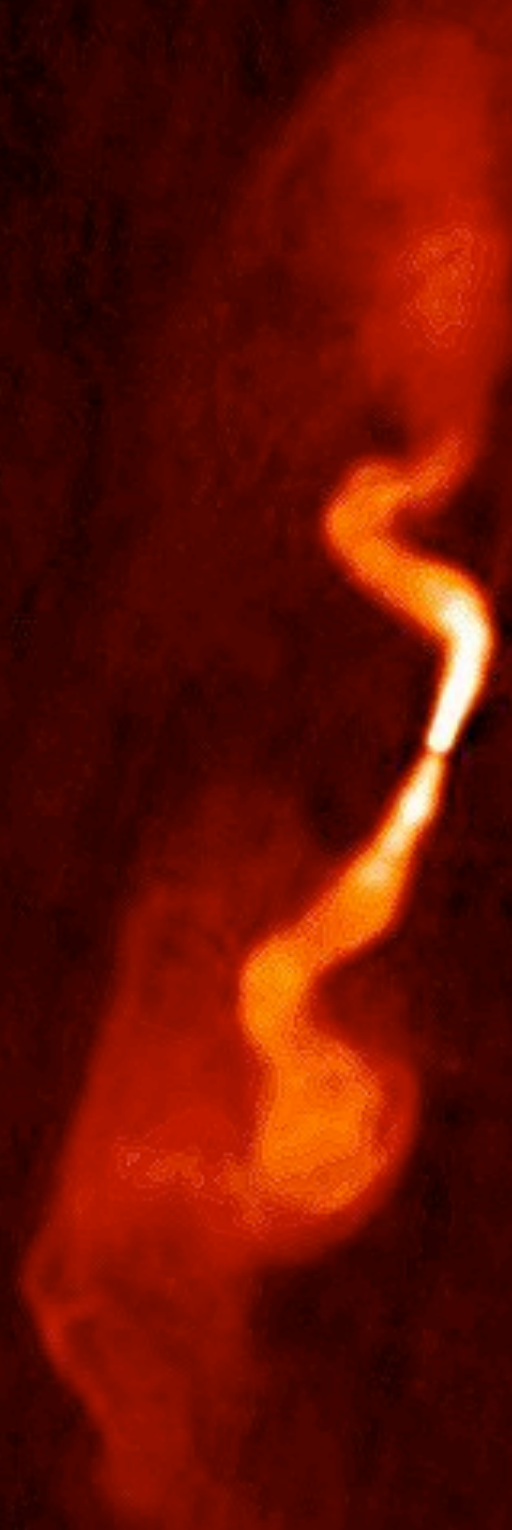
(* deconvolved)



1"

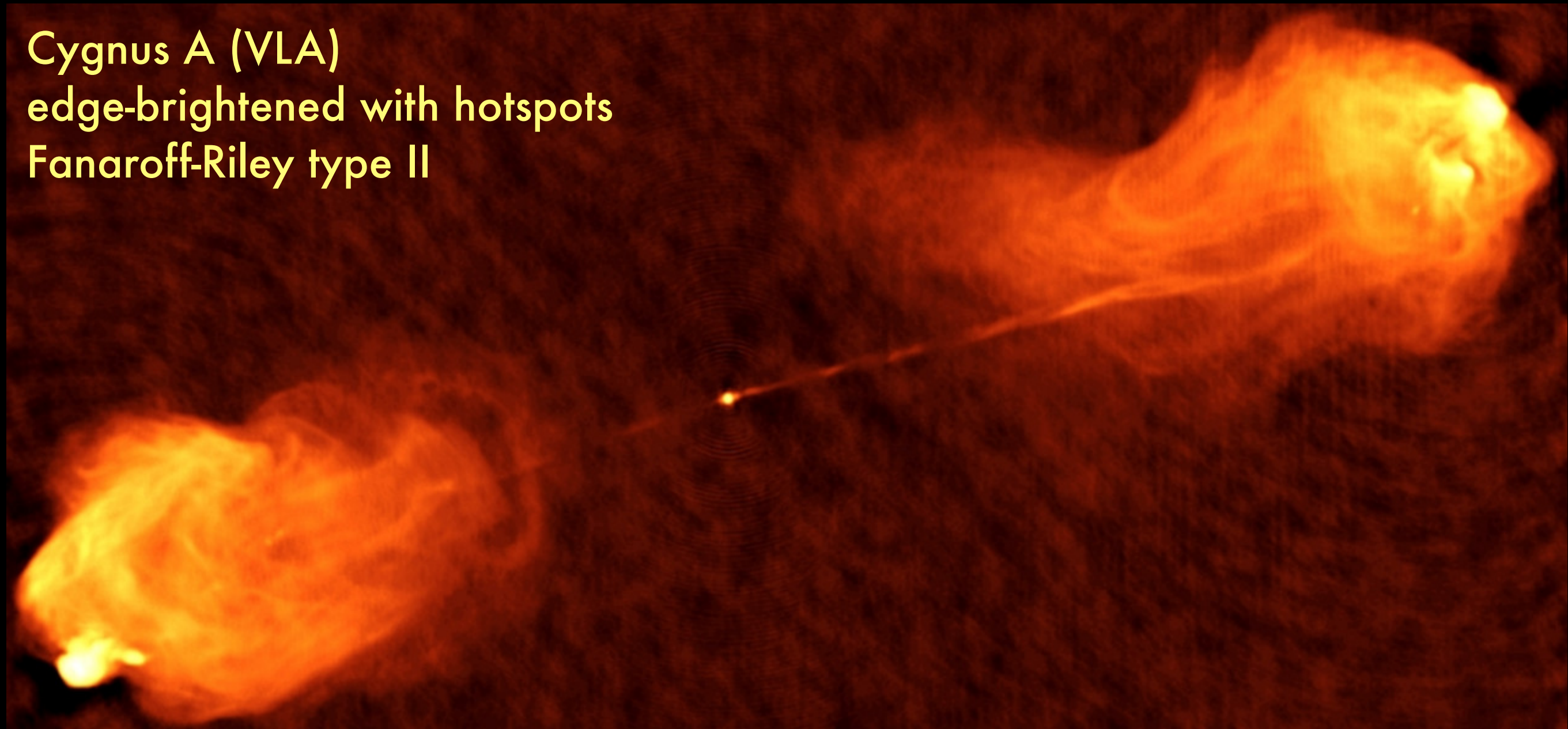
high-energy emission

low-energy emission

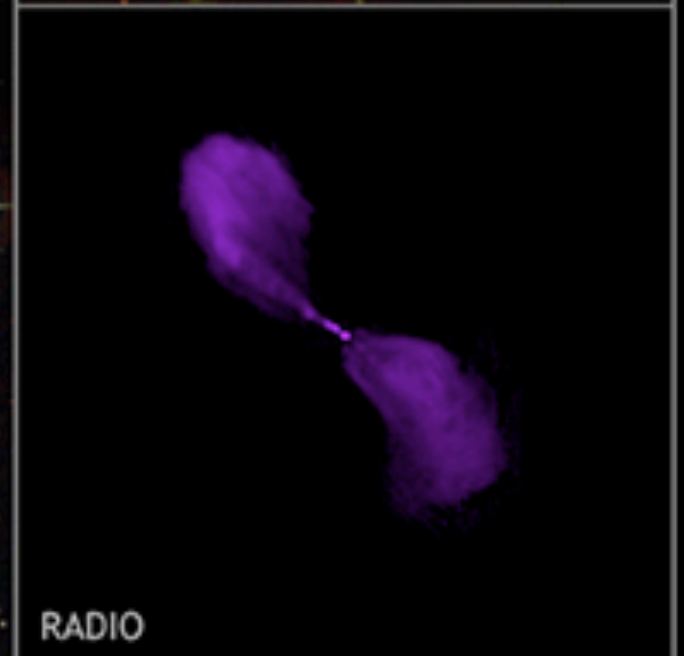
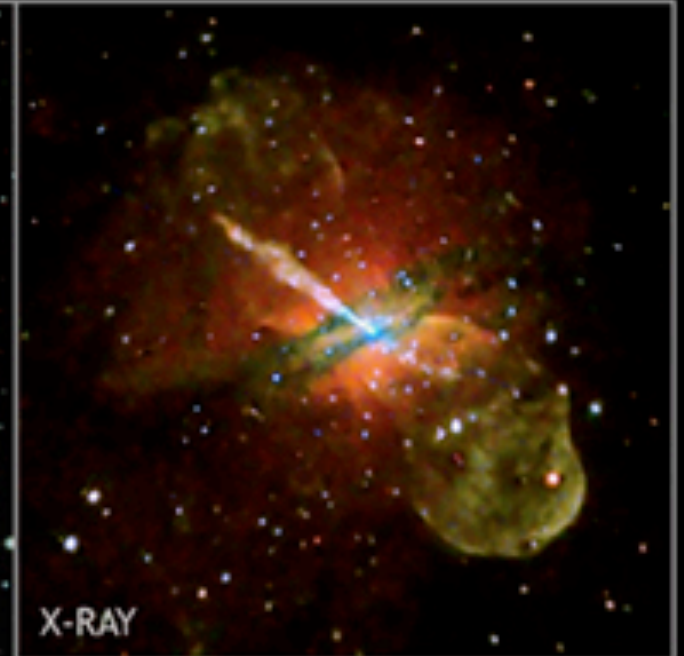
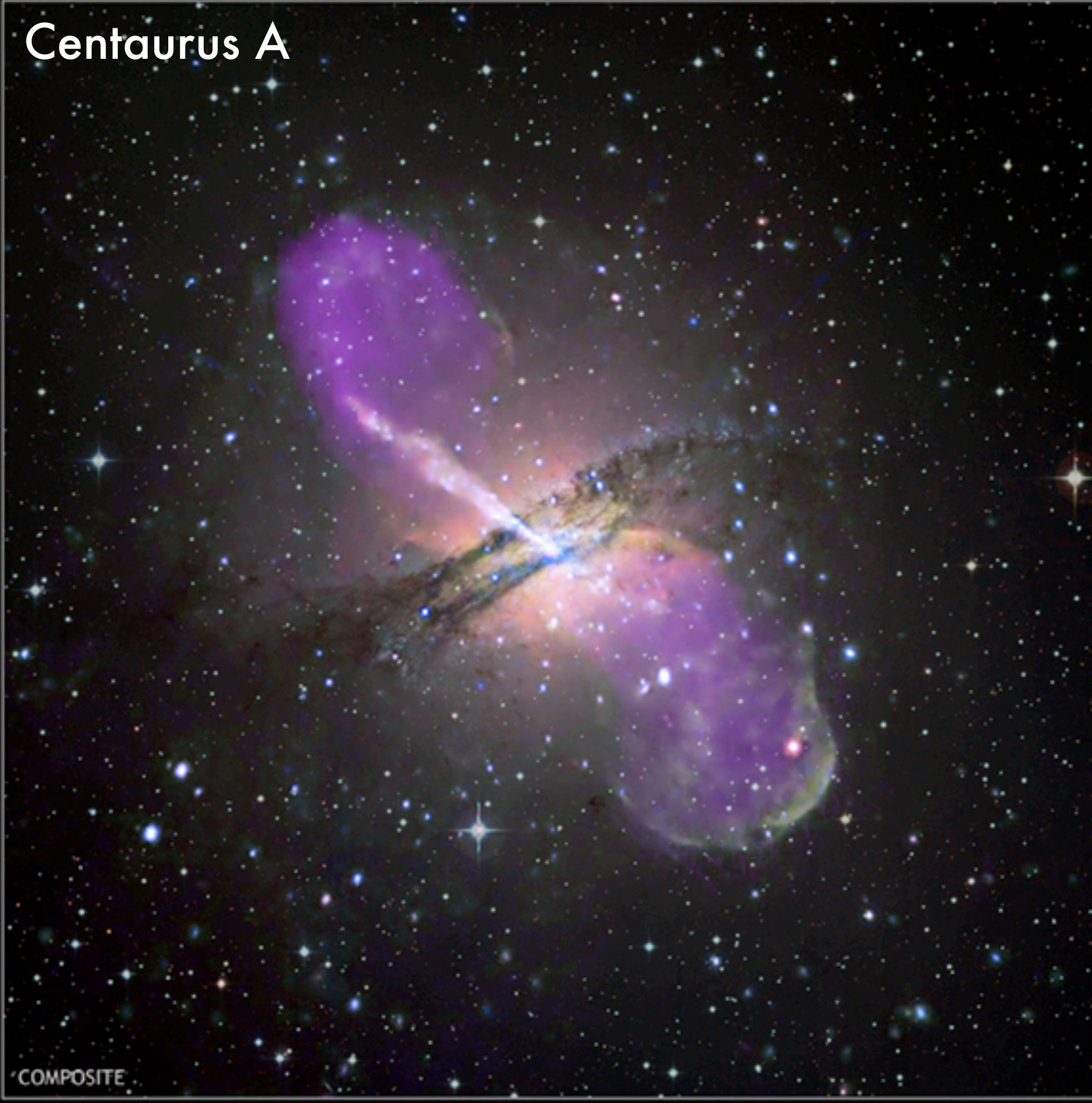


3C 31 (VLA)
center-brightened
Fanaroff-Riley type I

Cygnus A (VLA)
edge-brightened with hotspots
Fanaroff-Riley type II



Centaurus A



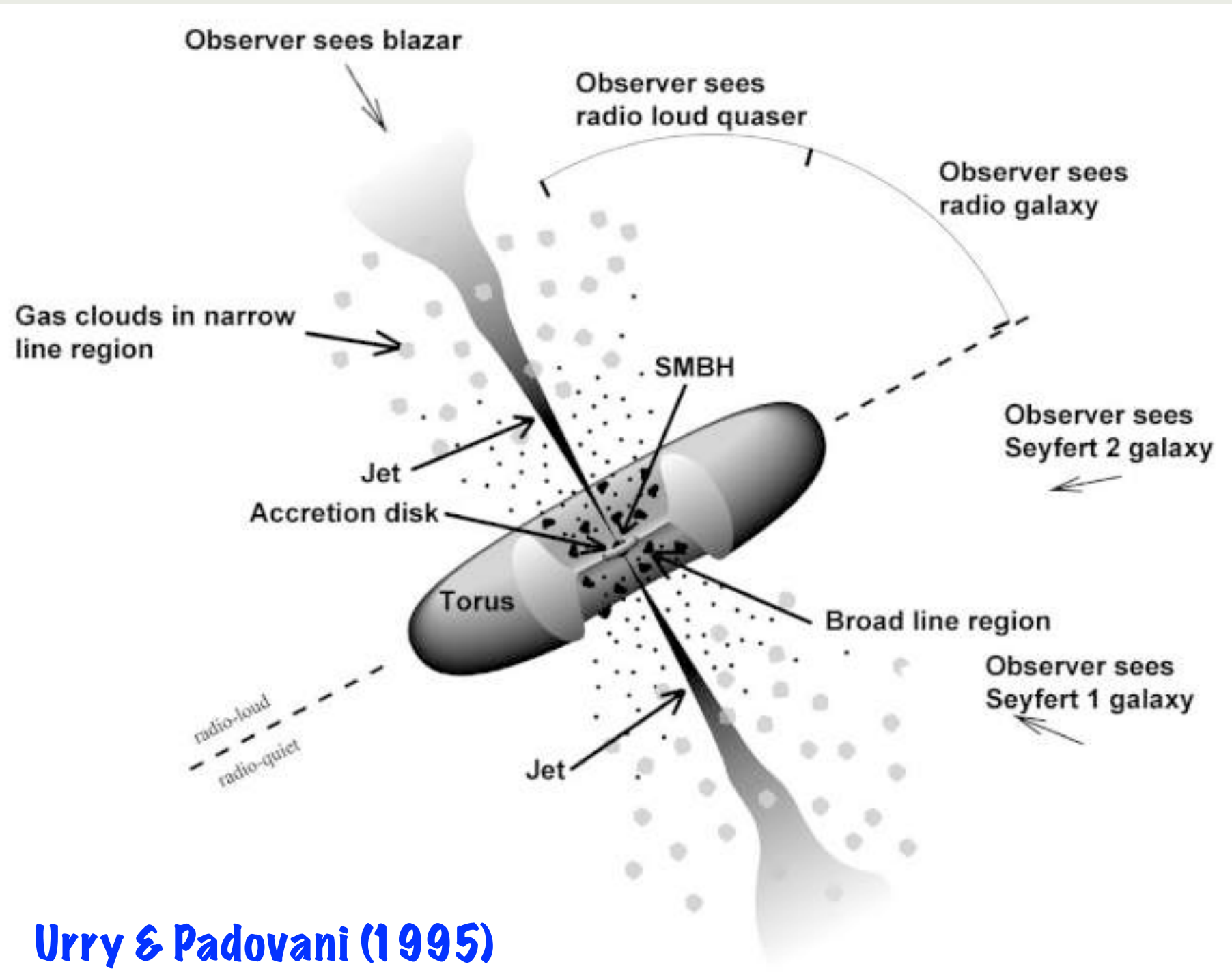
COMPOSITE

OPTICAL

X-RAY

RADIO

UNIFIED MODEL OF AGN



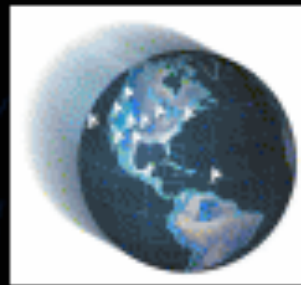
JETS FROM STELLAR MASS OBJECTS

SS433

VLBA

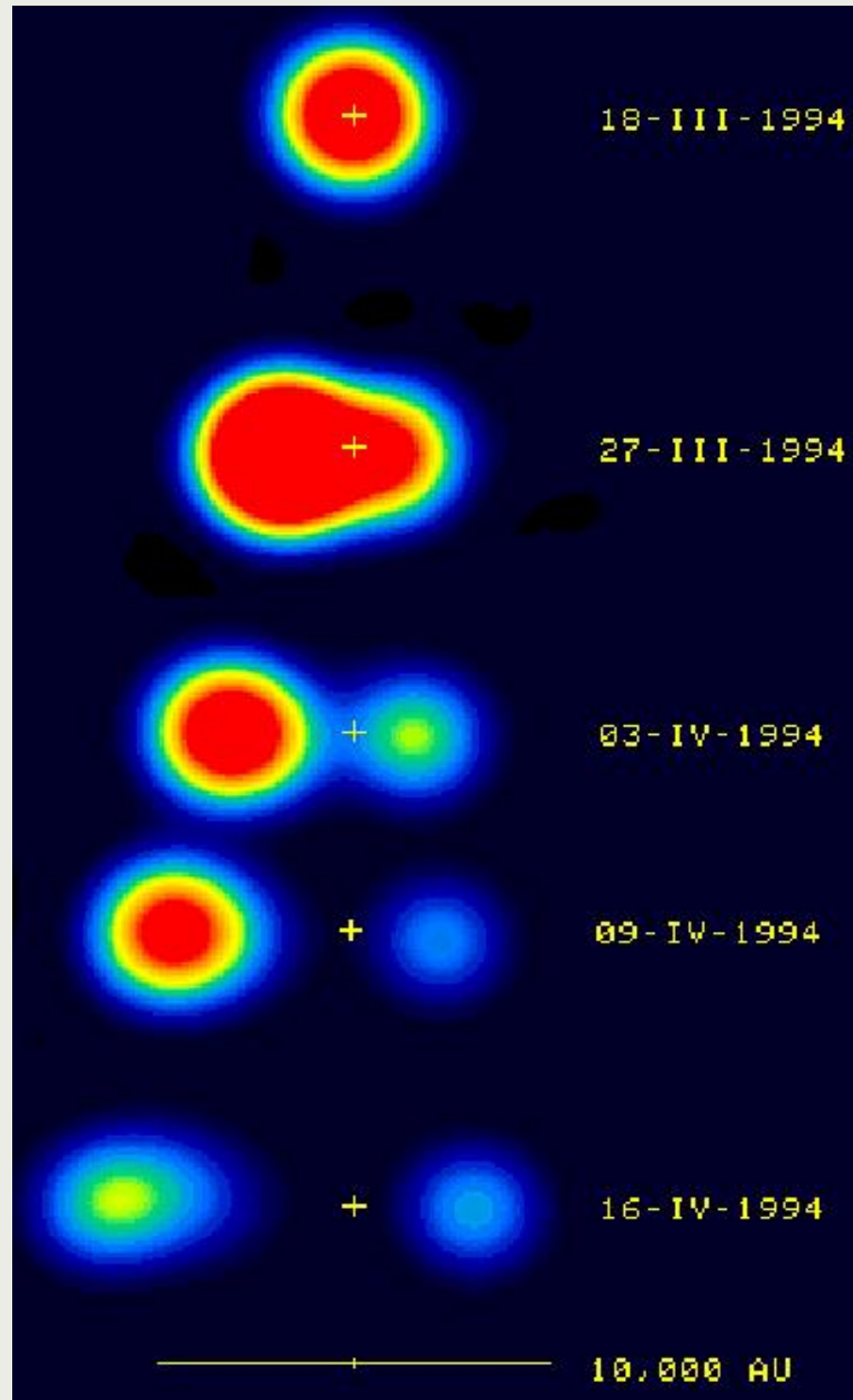


Amy Mioduszewski
Michael Rupen
Craig Walker
Greg Taylor

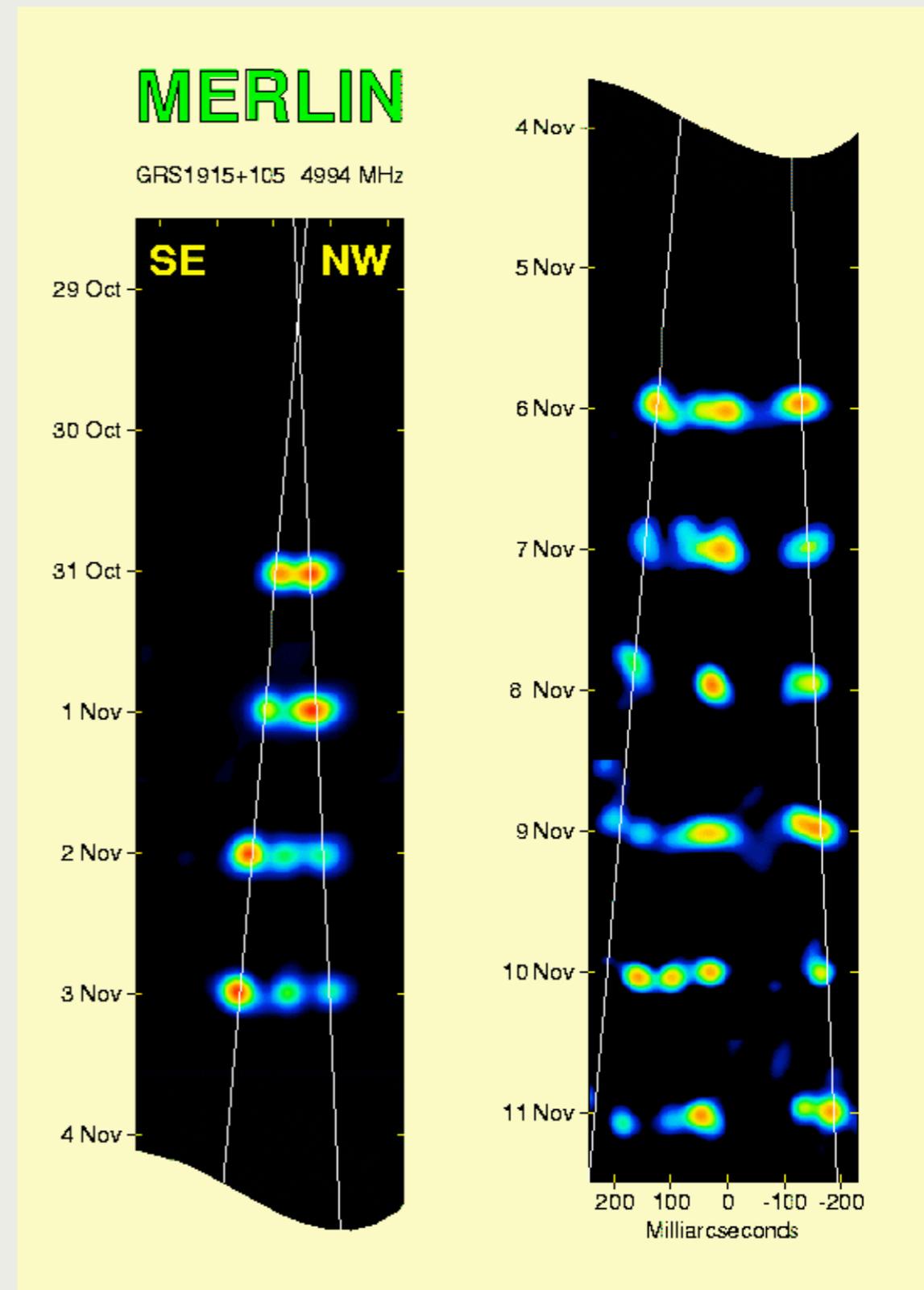


NRAO (2004)

GRS 1915+105

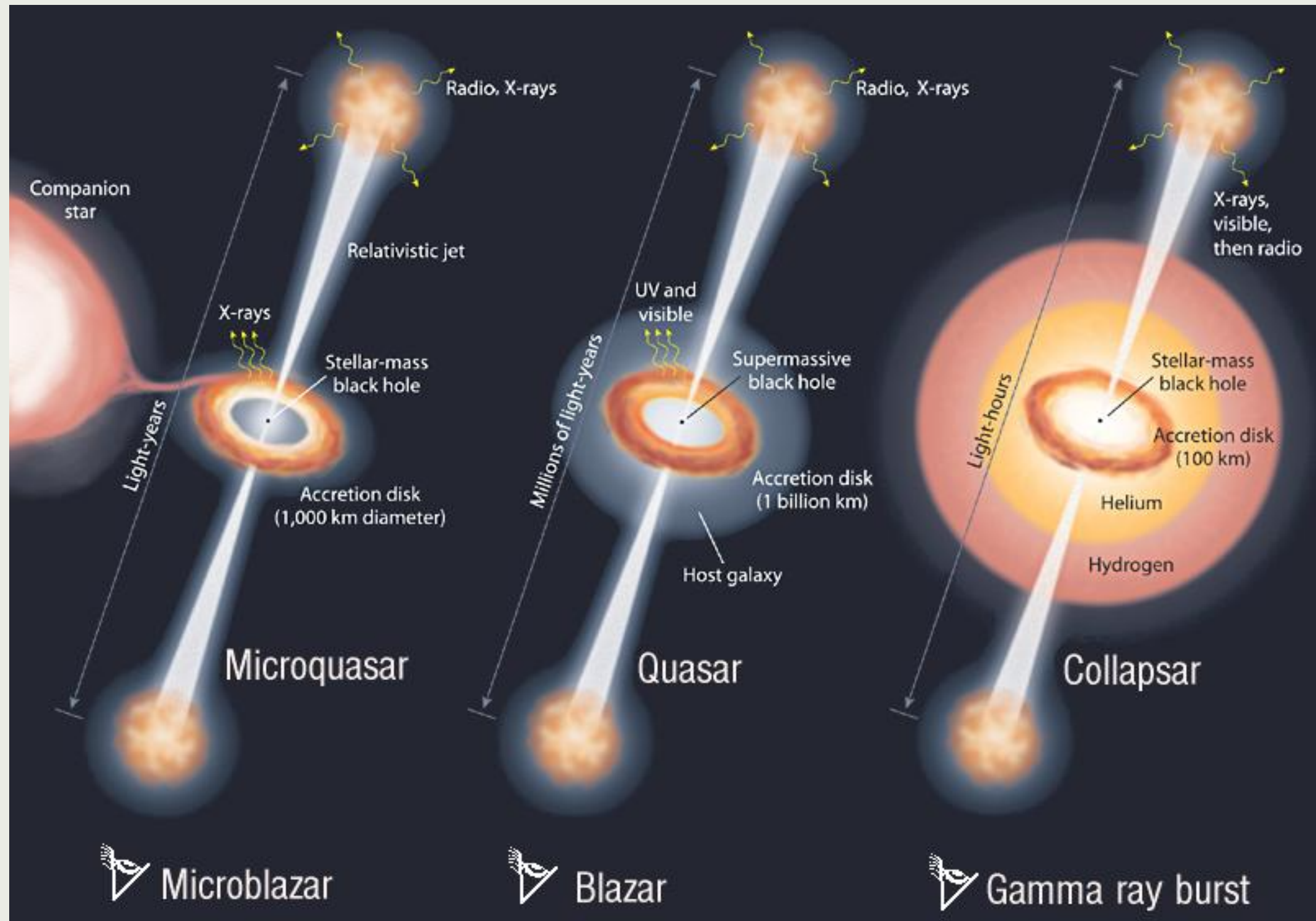


Mirabel & Rodriguez (1994)

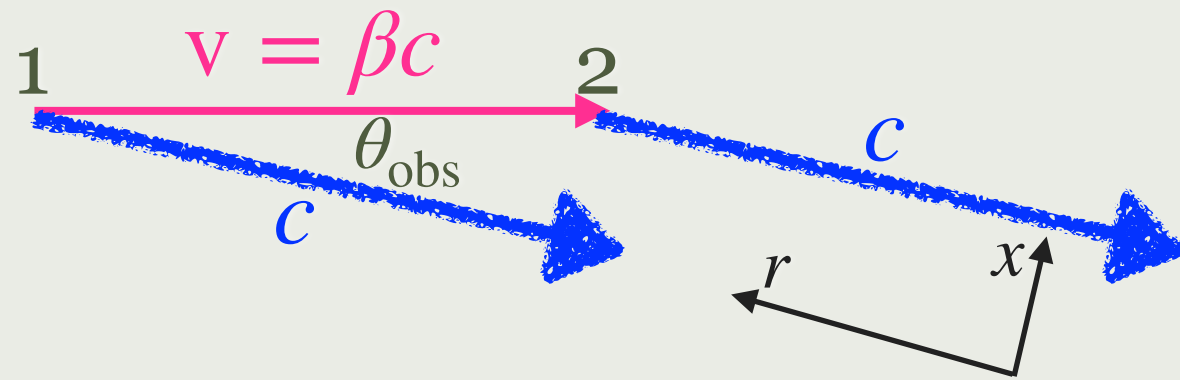


Fender et al. (1999)

RELATIVISTIC JETS FROM STELLAR-MASS OBJECTS

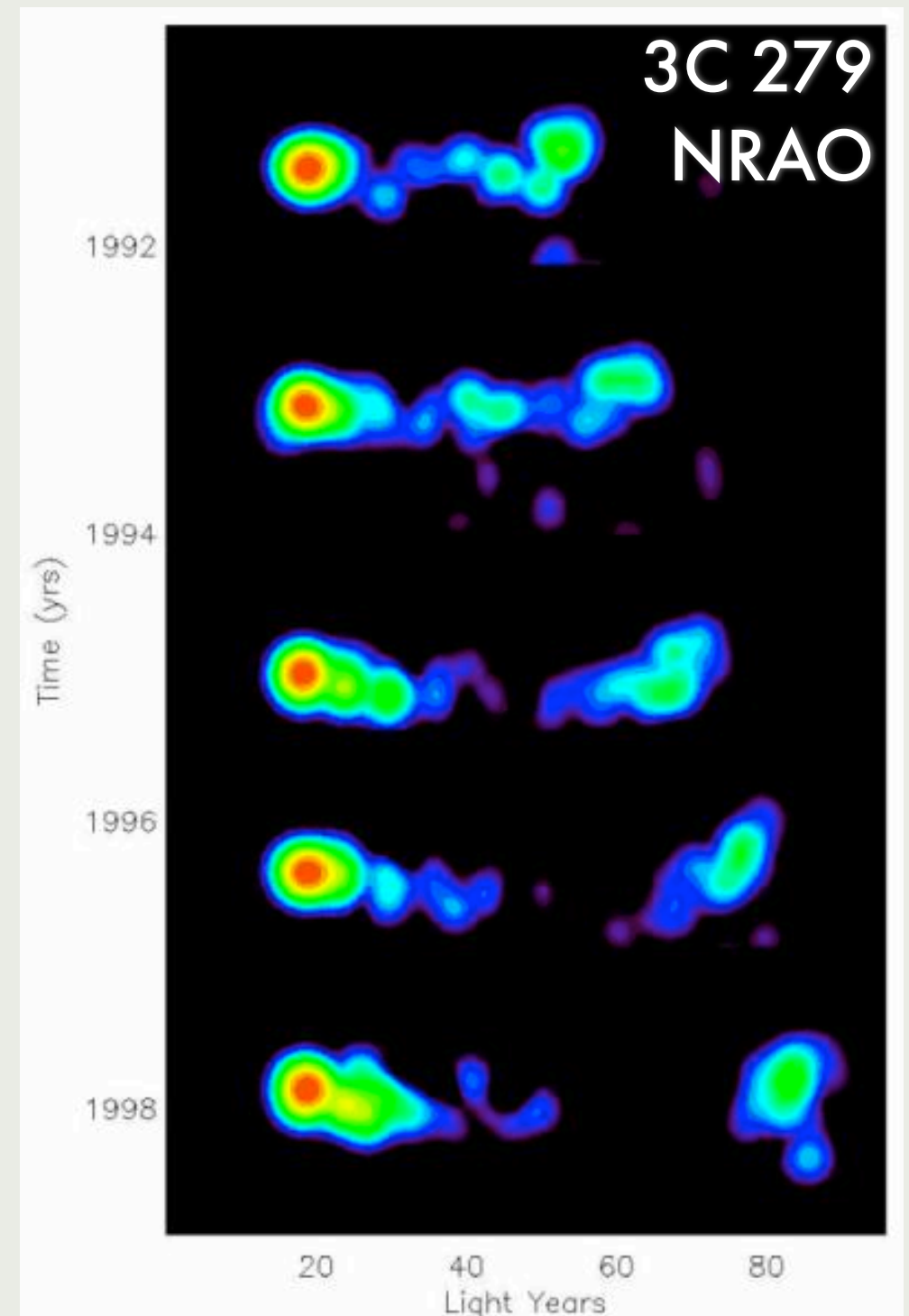


APPARENTLY SUPERLUMINAL MOTIONS

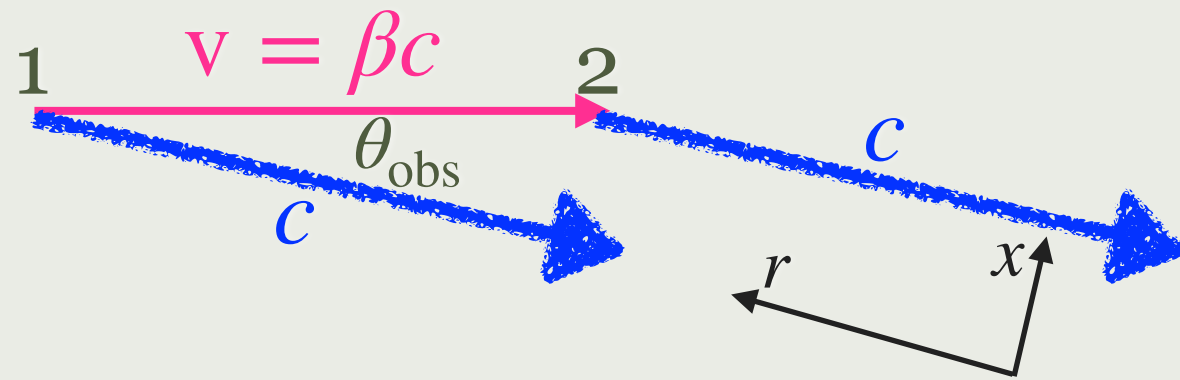


- A source moving with velocity \vec{v} emits two photons at time interval Δt_{em} in the same direction making with \vec{v} an angle θ_{obs} .
- The path of photon #2 is shifted from the path of photon #1 by $\Delta x = v \Delta t_{\text{em}} \sin \theta_{\text{obs}}$.
- Photon #1 is closer to the observer than photon #2 by $\Delta r = -(c - v \cos \theta_{\text{obs}}) \Delta t_{\text{em}}$, it will arrive earlier by $\Delta t_{\text{obs}} = -\Delta r/c = (1 - \beta \cos \theta_{\text{obs}}) \Delta t_{\text{em}}$.
- The apparent speed of the source is

$$v_{\text{app}} = \frac{\Delta x}{\Delta t_{\text{obs}}} = \frac{v \sin \theta_{\text{obs}}}{1 - \beta \cos \theta_{\text{obs}}}$$



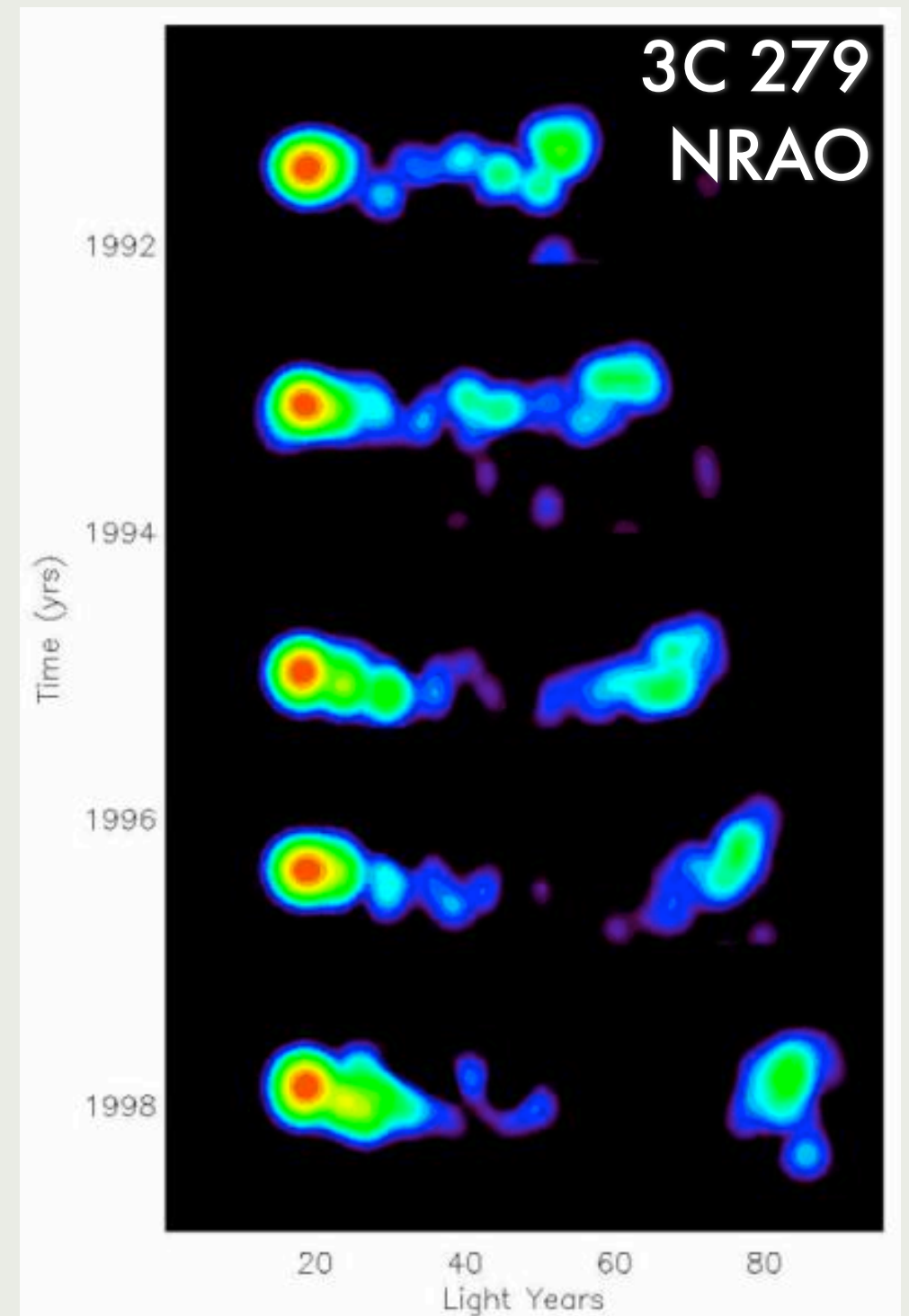
APPARENTLY SUPERLUMINAL MOTIONS



- The apparent speed of the source is

$$v_{\text{app}} = \frac{\Delta x}{\Delta t_{\text{obs}}} = \frac{v \sin \theta_{\text{obs}}}{1 - \beta \cos \theta_{\text{obs}}}$$

- Maximum value: $v_{\text{app}} = \Gamma v$
for the viewing angle satisfying $\sin \theta_{\text{obs}} = 1/\Gamma$ and $\cos \theta_{\text{obs}} = \beta$.
- Lower limit: $\Gamma > \beta_{\text{app}}$



RELATIVISTIC DOPPLER EFFECT

- We showed that $\Delta t_{\text{obs}} = (1 - \beta \cos \theta_{\text{obs}}) \Delta t_{\text{em}}$
(light-travel effect)

- The co-moving emission interval
(Lorentz transformation for $\Delta \vec{r}' = 0$):

$$\Delta t'_{\text{em}} = \frac{\Delta t_{\text{em}}}{\Gamma}$$

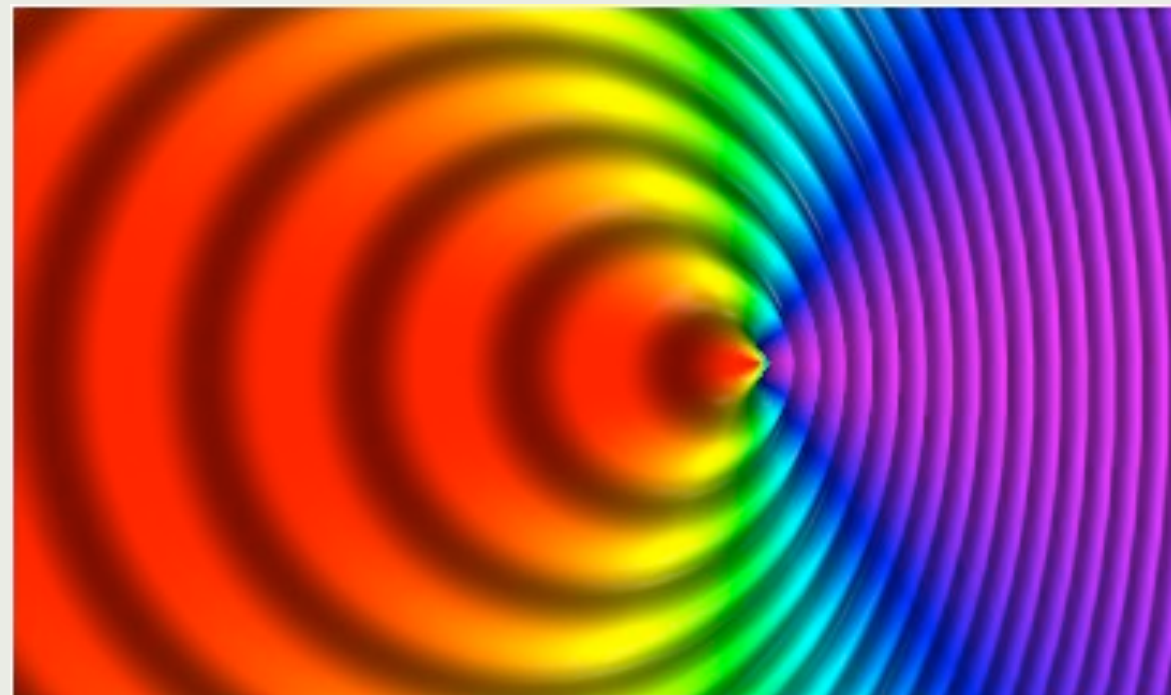
- frequency transformation:

$$\frac{\nu_{\text{obs}}}{\nu'_{\text{em}}} = \frac{\Delta t'_{\text{em}}}{\Delta t_{\text{obs}}} = \frac{1}{\Gamma(1 - \beta \cos \theta_{\text{obs}})} \equiv \mathcal{D}$$

the relativistic Doppler factor

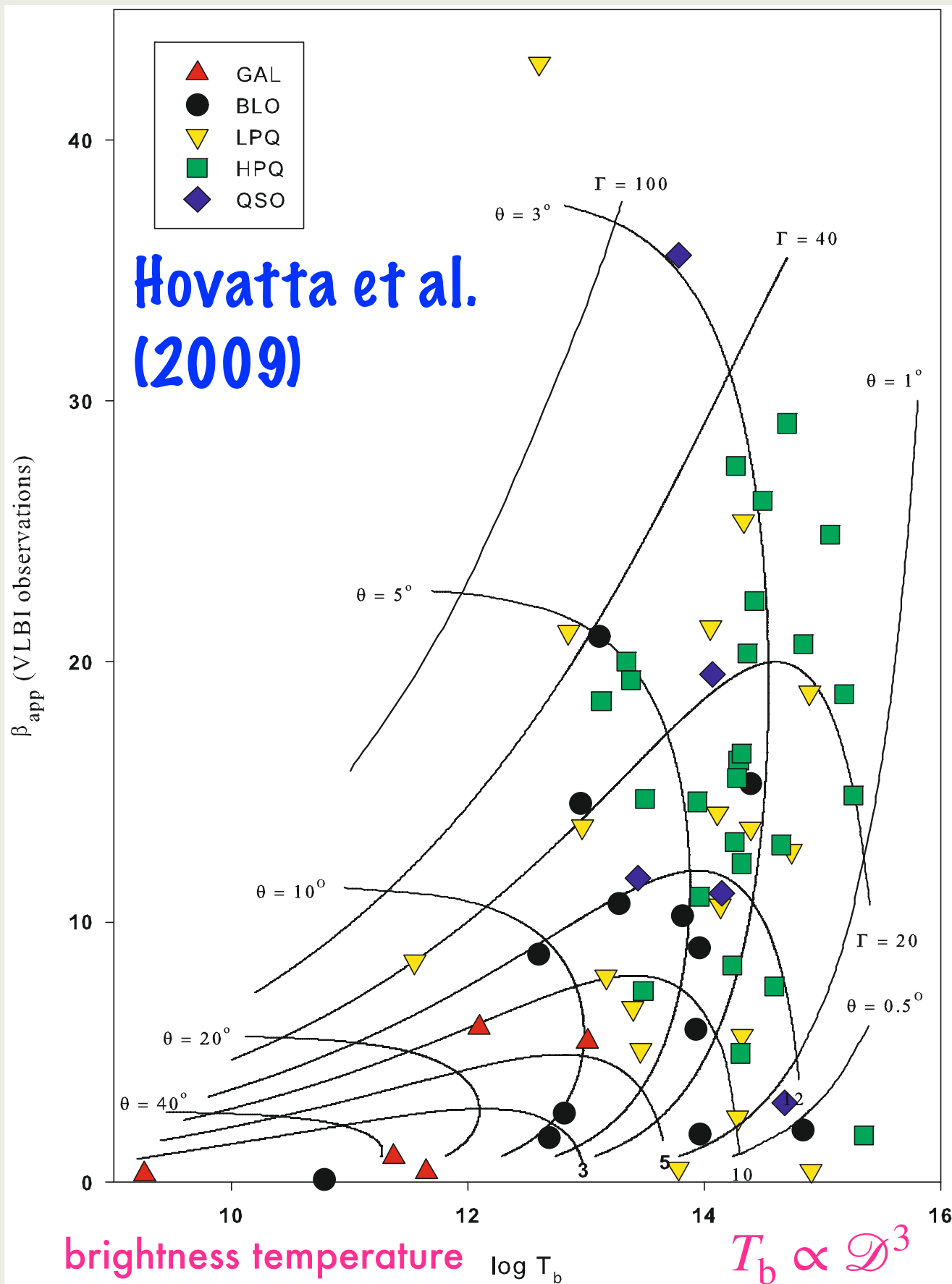
- for $\cos \theta_{\text{obs}} = \beta$: $\mathcal{D} = \frac{1}{\Gamma(1 - \beta^2)} = \Gamma$

a source moving to the right with $v = 0.7c$



en:TxAlien, CC BY-SA 3.0, Wikimedia Commons

SUPERLUMINAL MOTIONS AND DOPPLER EFFECT



- For some blazars it is possible to independently determine apparent speed $\beta_{\text{app}} = v_{\text{app}}/c$ and Doppler factor \mathcal{D} .

- Inverting the relations

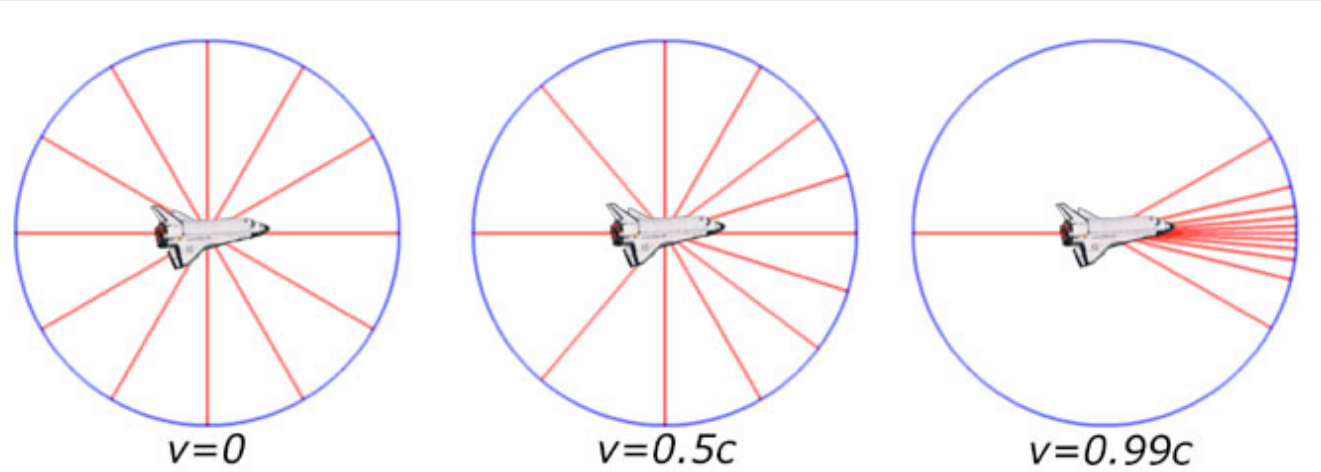
$$\beta_{\text{app}} = \frac{\beta \sin \theta_{\text{obs}}}{1 - \beta \cos \theta_{\text{obs}}} \text{ and}$$

$$\mathcal{D} = \frac{1}{\Gamma(1 - \beta \cos \theta_{\text{obs}})}:$$

$$\Gamma = \frac{\mathcal{D}^2 + \beta_{\text{app}}^2 + 1}{2\mathcal{D}} \text{ and}$$

$$\tan \theta_{\text{obs}} = \frac{2\beta_{\text{app}}}{\mathcal{D}^2 + \beta_{\text{app}}^2 - 1}$$

RELATIVISTIC ABERRATION



Brandeker
(2002)

$\Gamma = 1$

$\Gamma \simeq 1.15$

$\Gamma \simeq 7.1$

synchrotron radiation

- solid angle transformation:

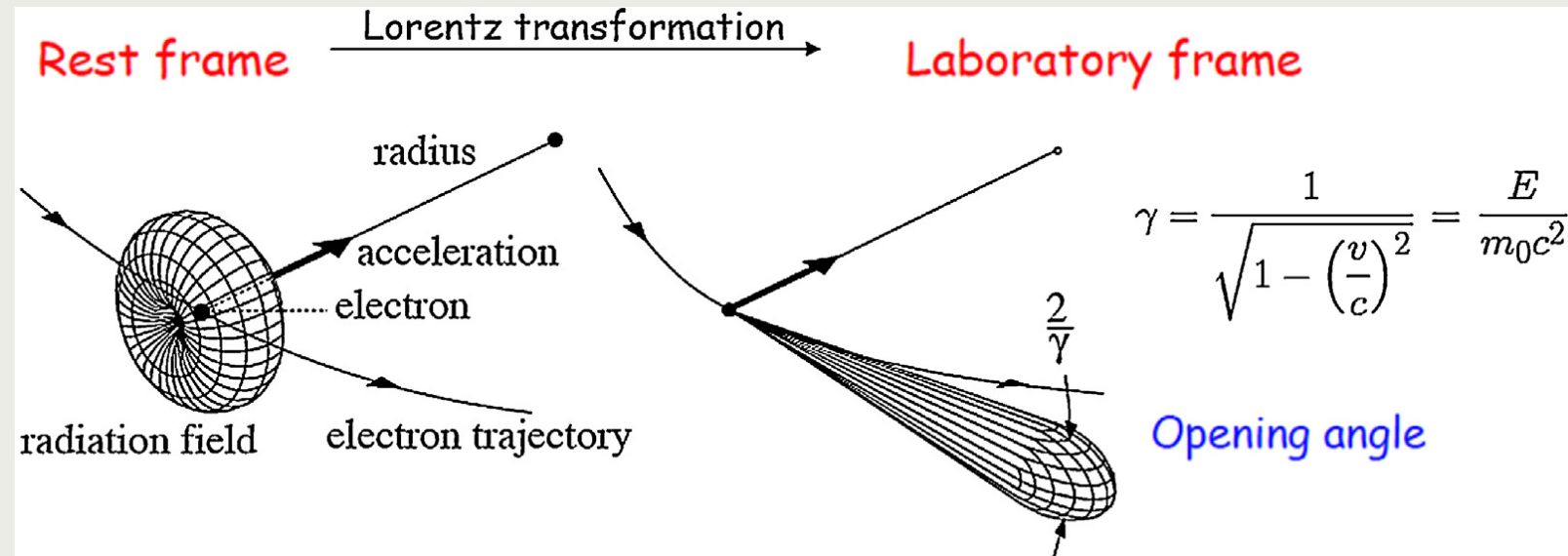
$$\Delta\Omega_{\text{obs}} = \frac{\Delta\Omega'_{\text{em}}}{\mathcal{D}^2}$$

- intensity transformation:

$$\frac{I_\nu}{\nu^3} = \text{const}, \text{ hence } I_{\nu,\text{obs}} = \mathcal{D}^3 I'_{\nu,\text{em}}$$

- luminosity transformation:

$$L = \int L_\nu d\nu \propto \nu^4, \text{ hence } L_{\text{obs}} = \mathcal{D}^4 L'_{\text{em}}$$



$$\gamma = \frac{1}{\sqrt{1 - \left(\frac{v}{c}\right)^2}} = \frac{E}{m_0 c^2}$$

Opening angle

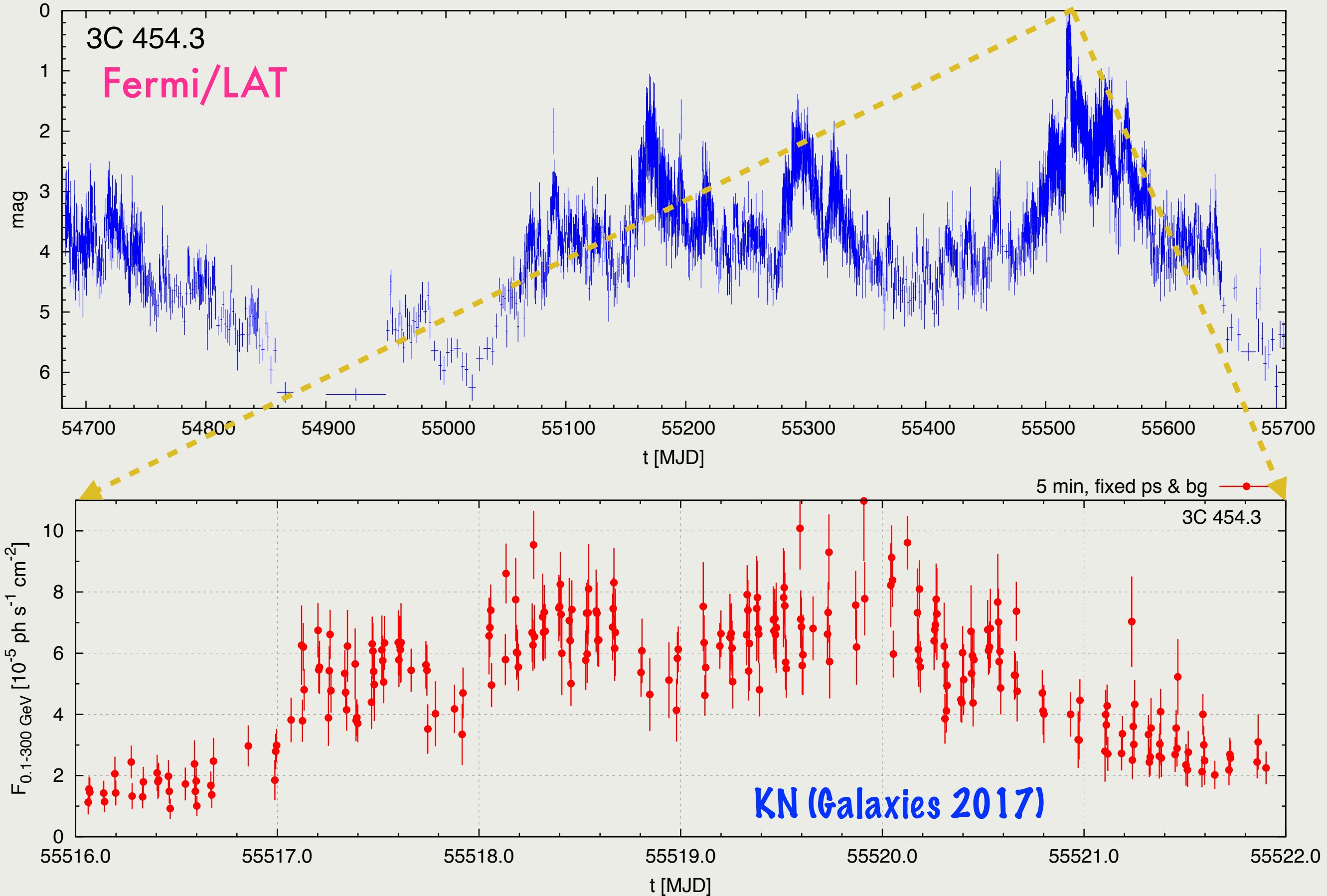
Eberhardt (2015)

for $\mathcal{D} \simeq \Gamma \sim 10$:

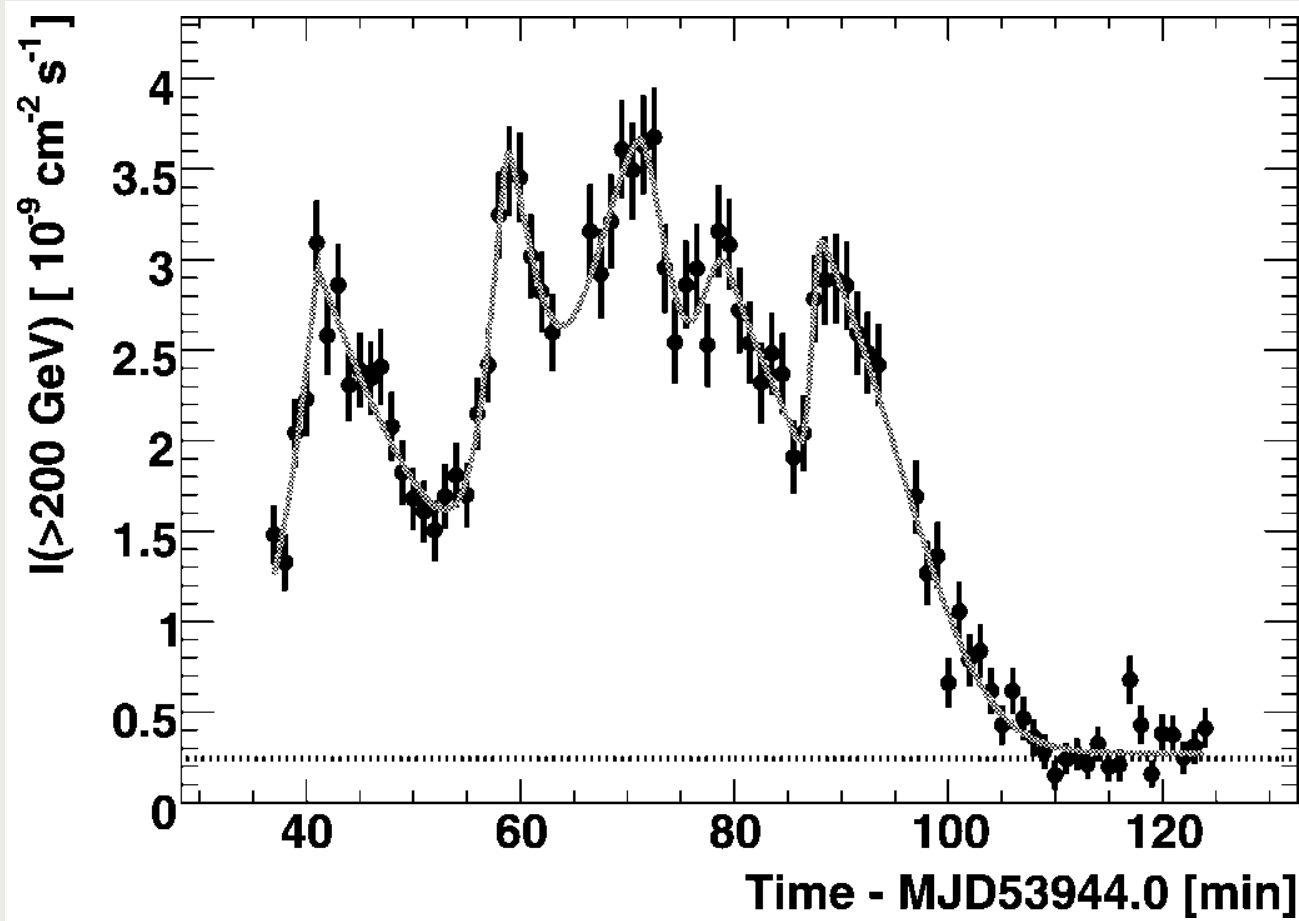
$$L_{\text{obs}} \sim 10^4 L'_{\text{em}} (!)$$

BLAZARS

GAMMA-RAY VARIABILITY OF BLAZARS



SHORTEST VARIABILITY TIME SCALES



PKS 2155-304
H.E.S.S. Collaboration (2007)

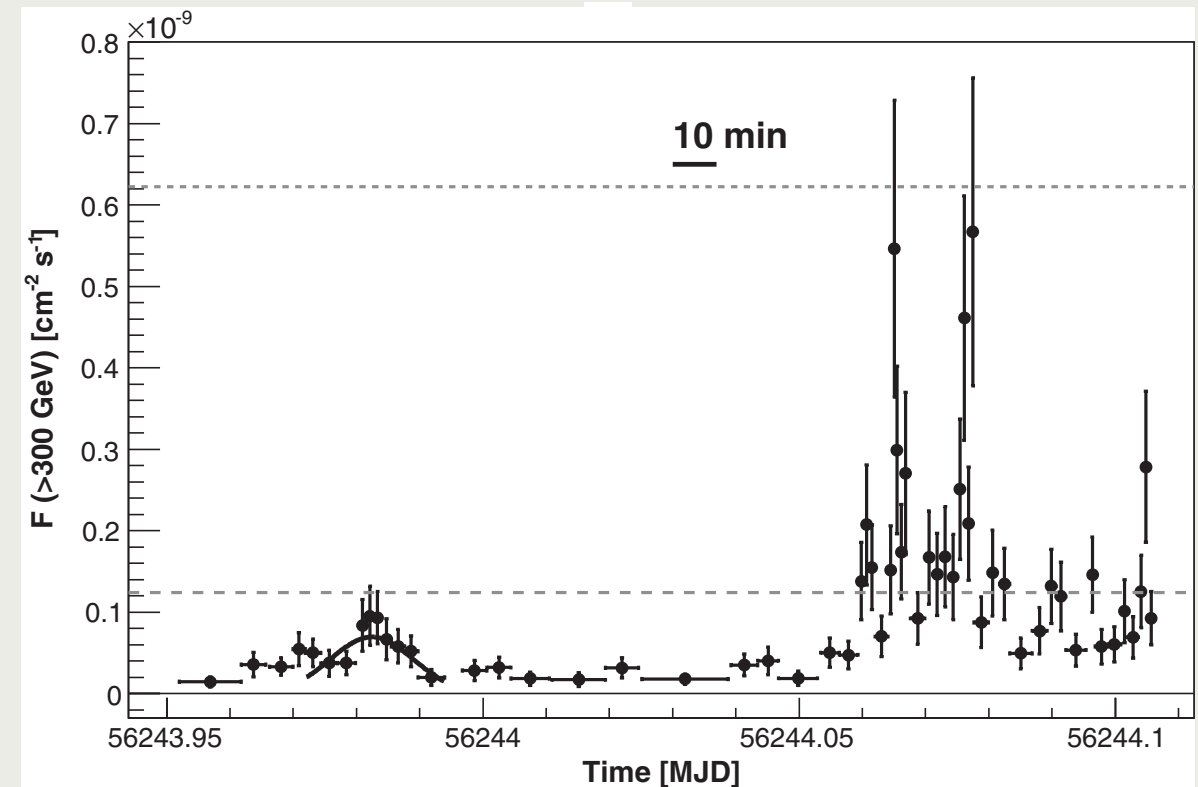
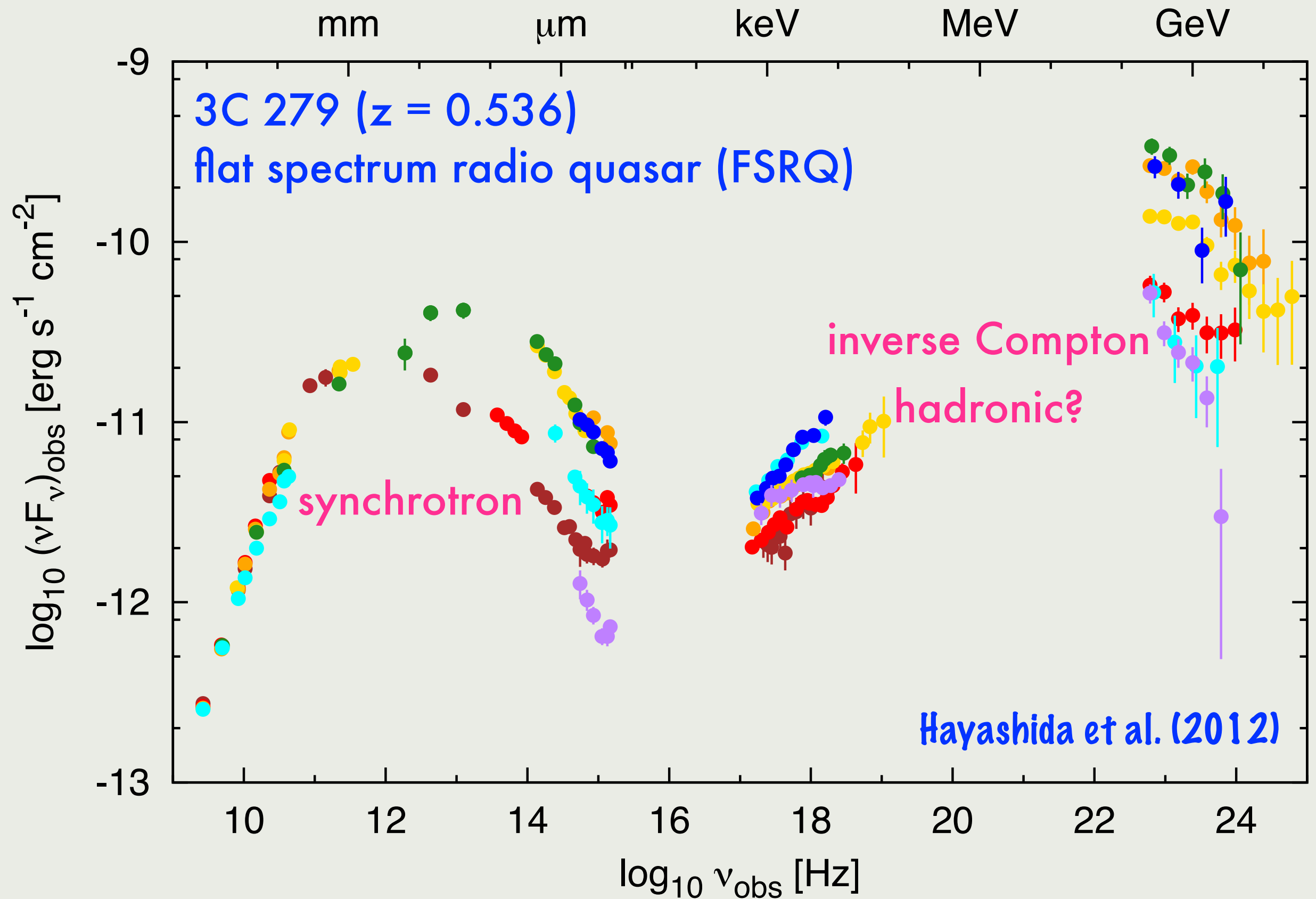


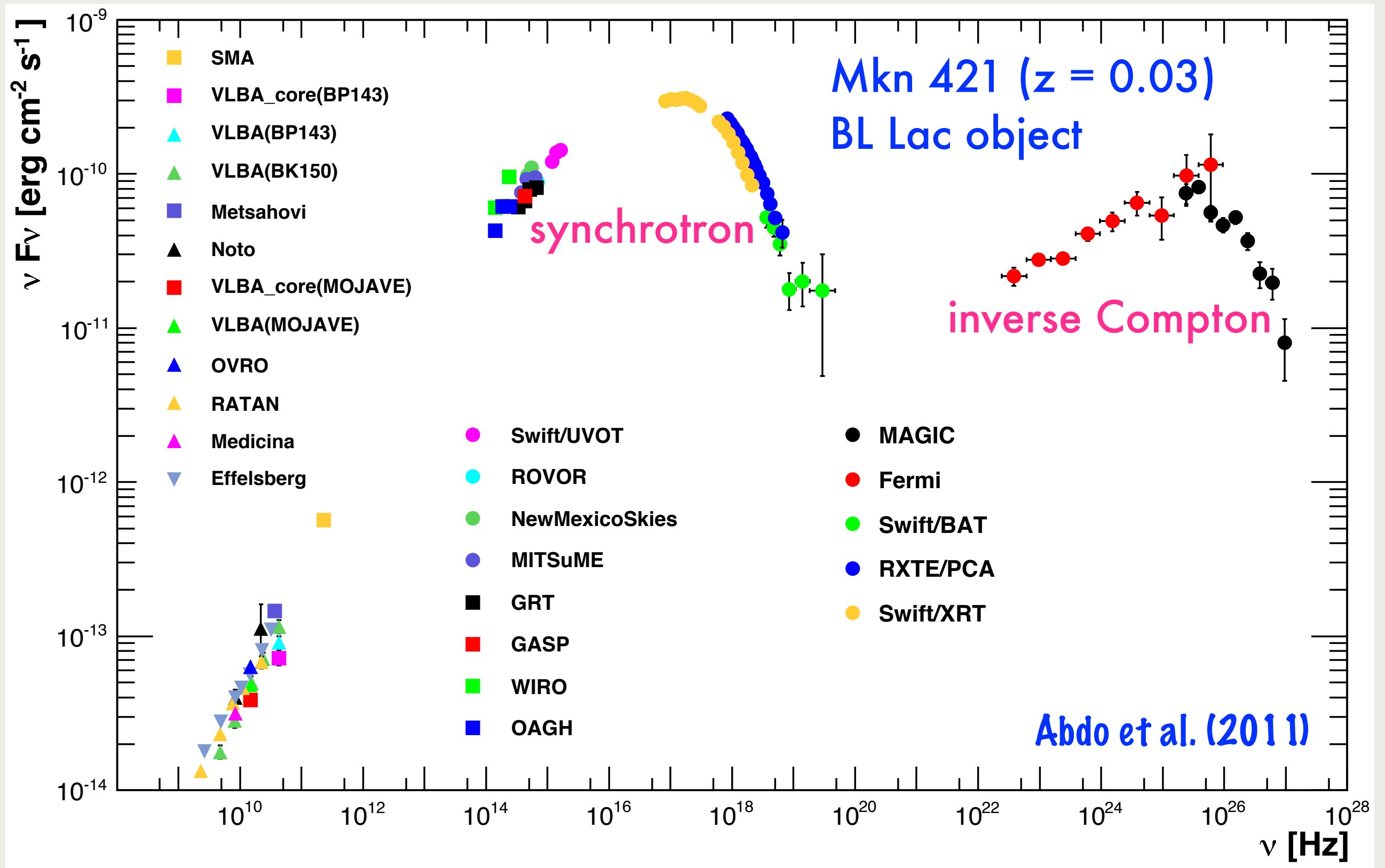
Fig. 4. Light curve of IC 310 observed with the MAGIC telescopes on the night of 12/13 November 2012, above 300 GeV. As a flux reference, the two gray lines indicate levels of 1 and 5 times the flux level of the Crab Nebula, respectively. The precursor flare (MJD 56243.972-56243.994) has been fitted with a Gaussian distribution. Vertical error bars show 1 SD statistical uncertainty. Horizontal error bars show the bin widths.

IC 310
MAGIC Collaboration (2014)

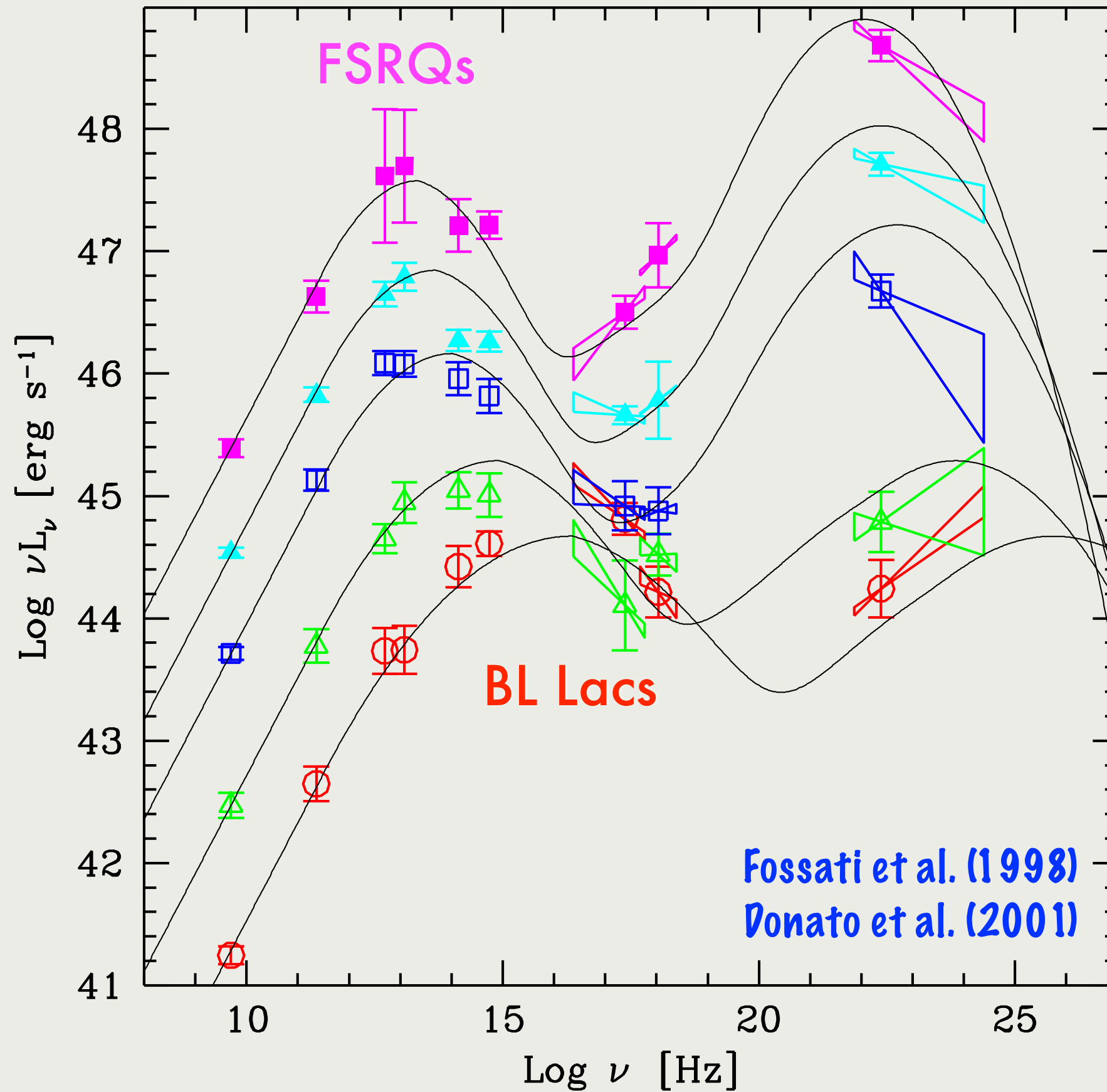
SPECTRAL ENERGY DISTRIBUTION OF A LUMINOUS BLAZAR



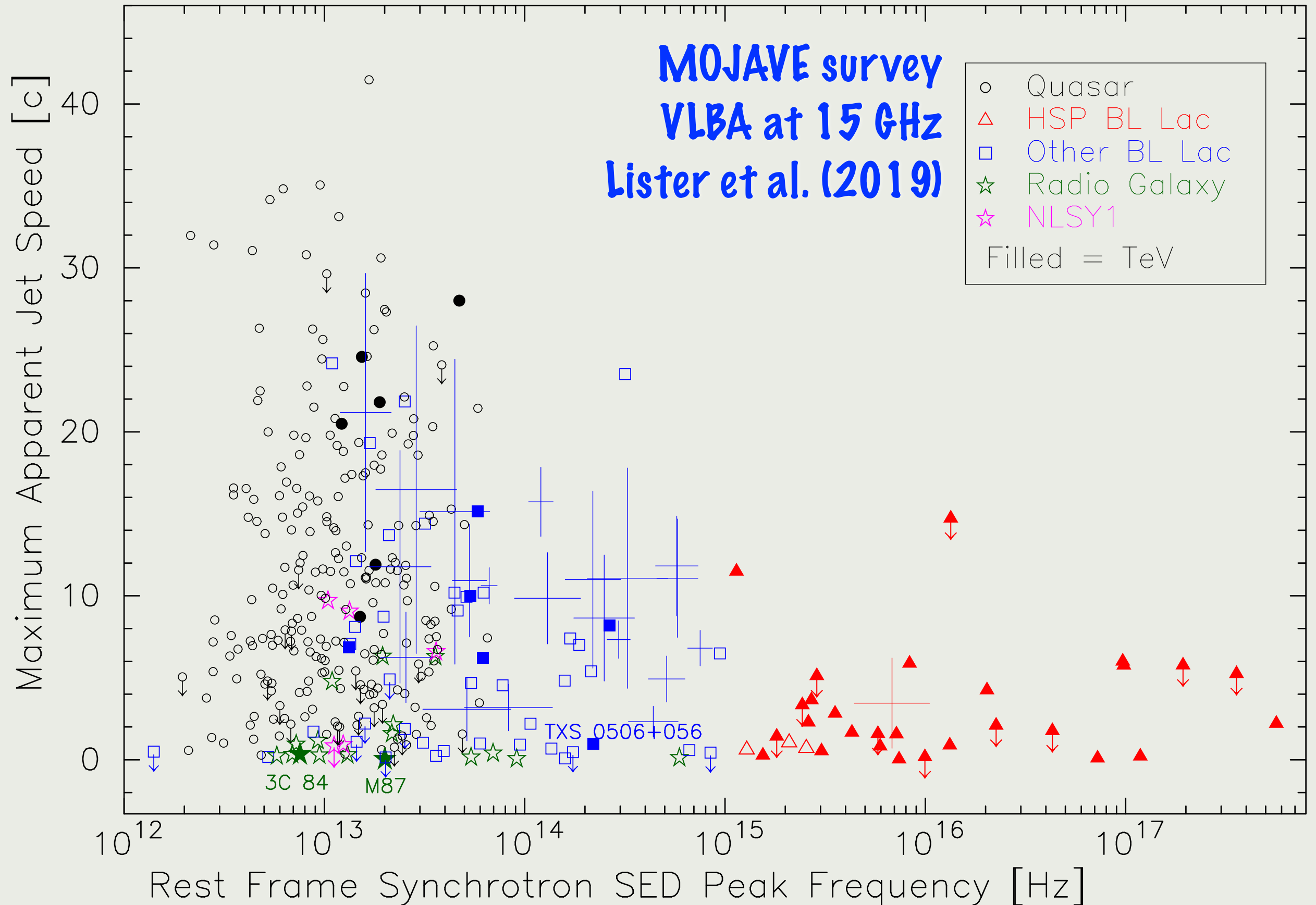
SPECTRAL ENERGY DISTRIBUTION OF A LOW-LUMINOSITY BLAZAR



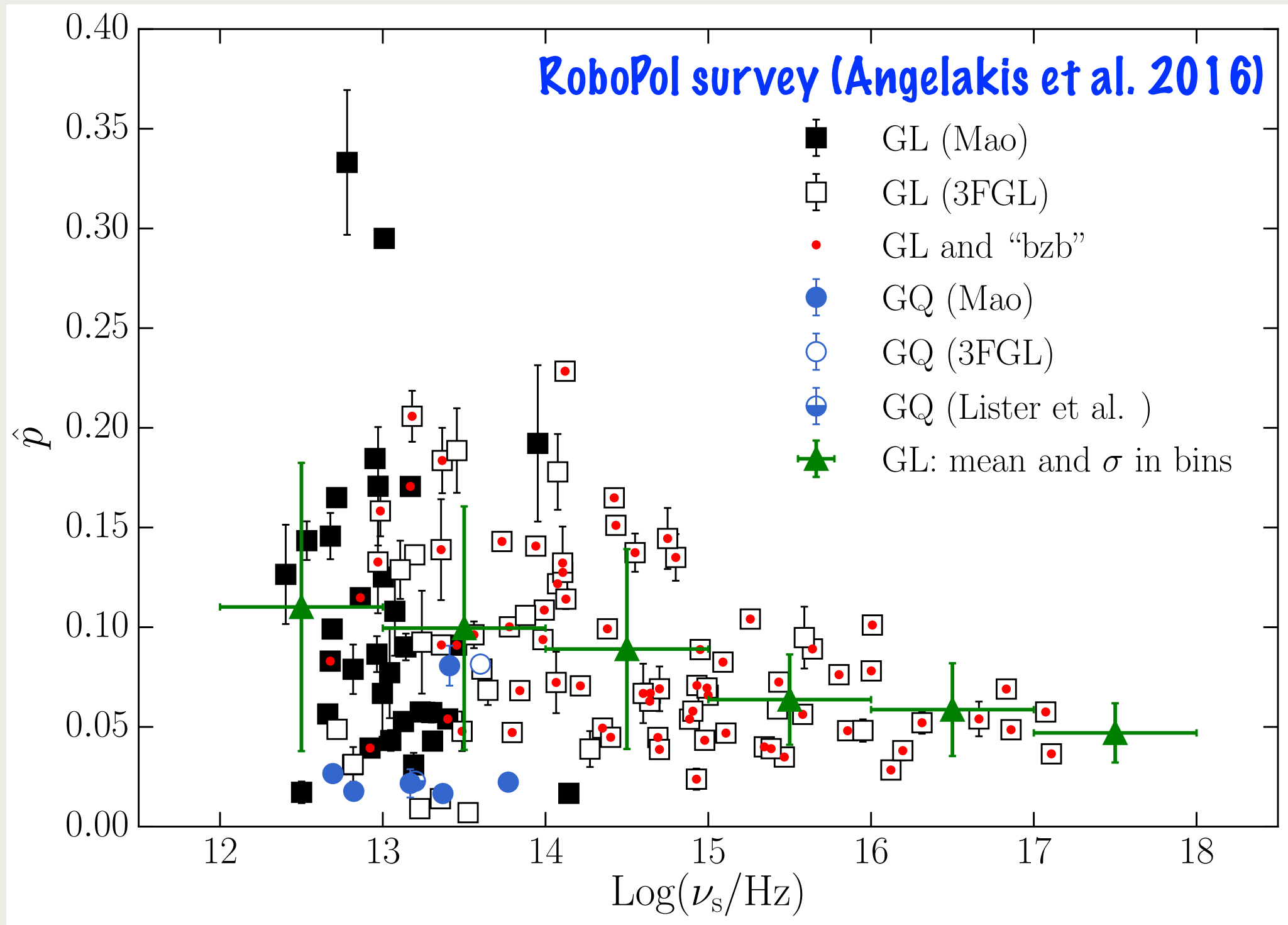
BLAZAR SEQUENCE



BLAZAR SEQUENCE: SUPERLUMINAL MOTIONS

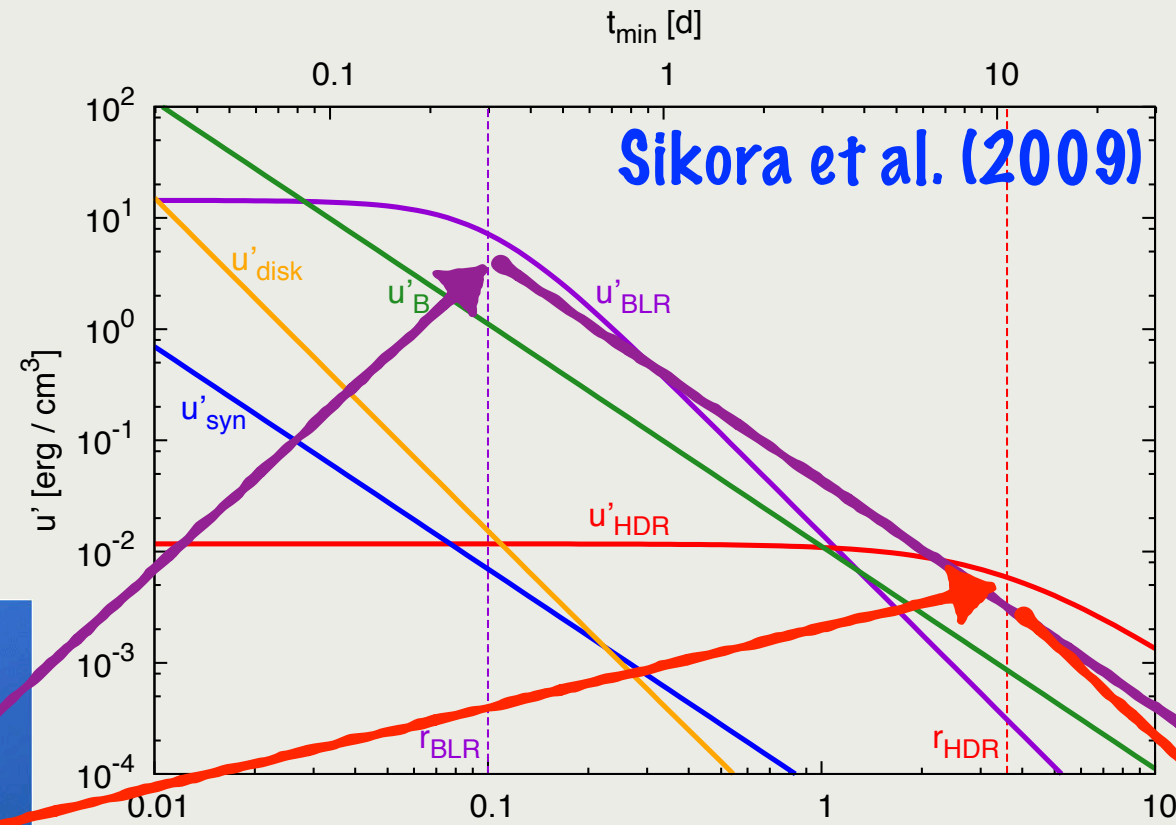
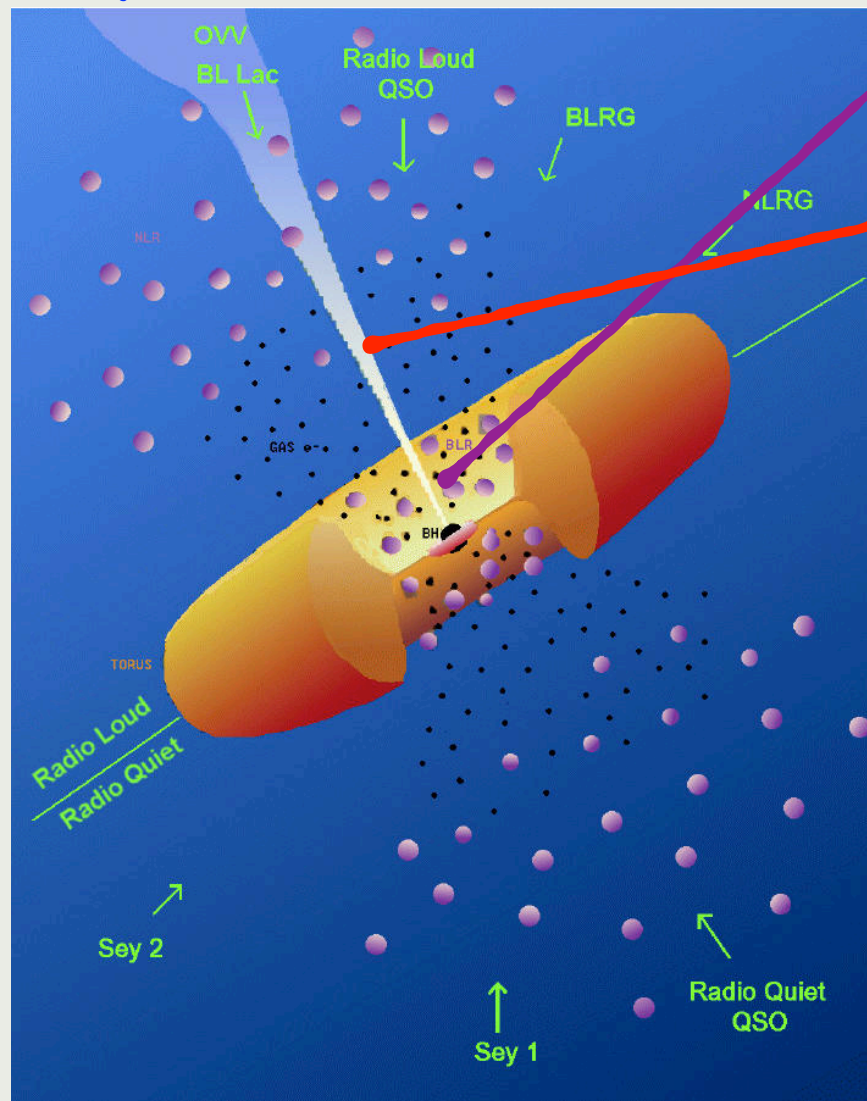


BLAZAR SEQUENCE: OPTICAL POLARIZATION



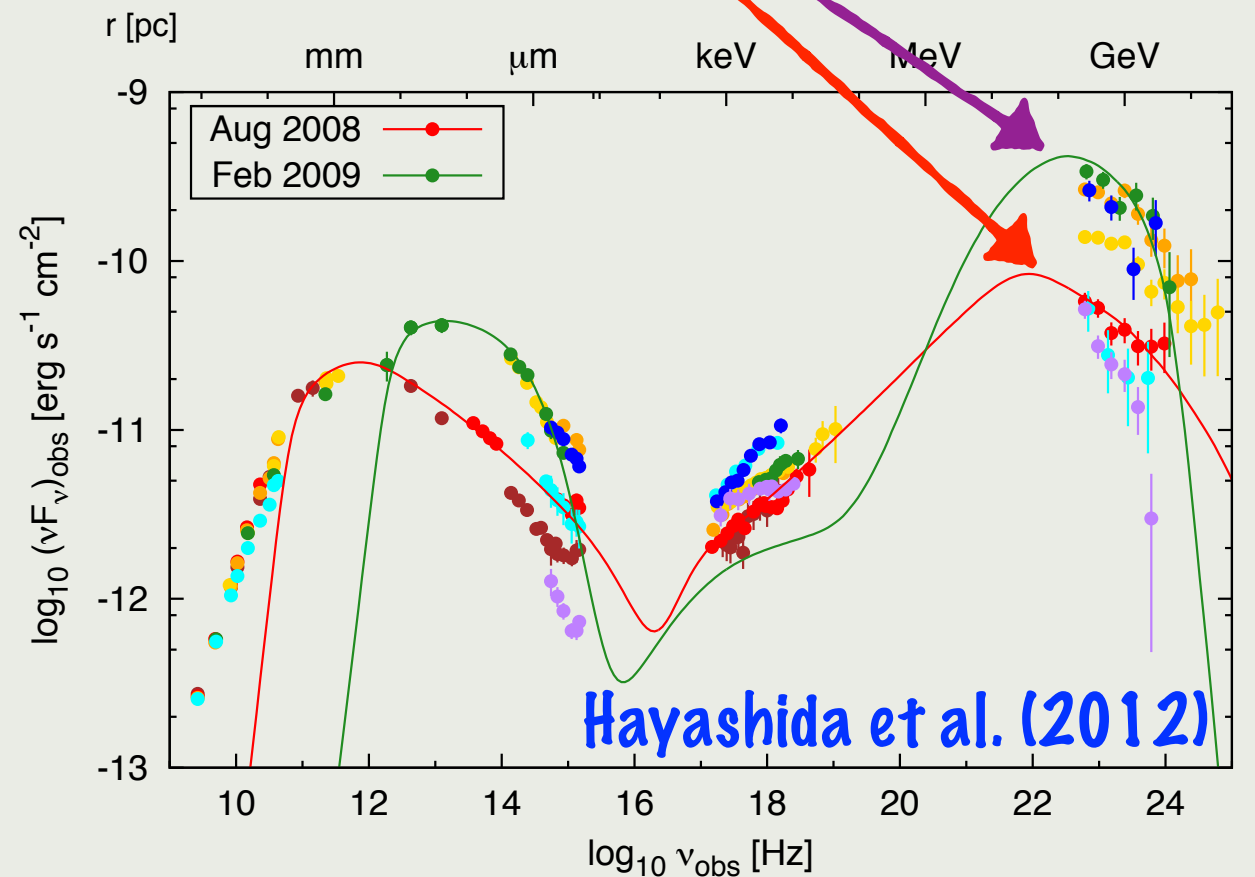
MAGNETIC FIELD STRENGTH FROM SYNCHROTRON LUMINOSITY

Urry & Padovani (1995)



$$\frac{L_{\text{syn}}}{L_{\text{IC}}} \simeq \frac{u'_B}{u'_{\text{ext}}}$$

$$u'_{\text{ext}} \sim \frac{\xi \Gamma_j^2 L_{\text{acc}}}{4\pi c r_{\text{ext}}^2}$$

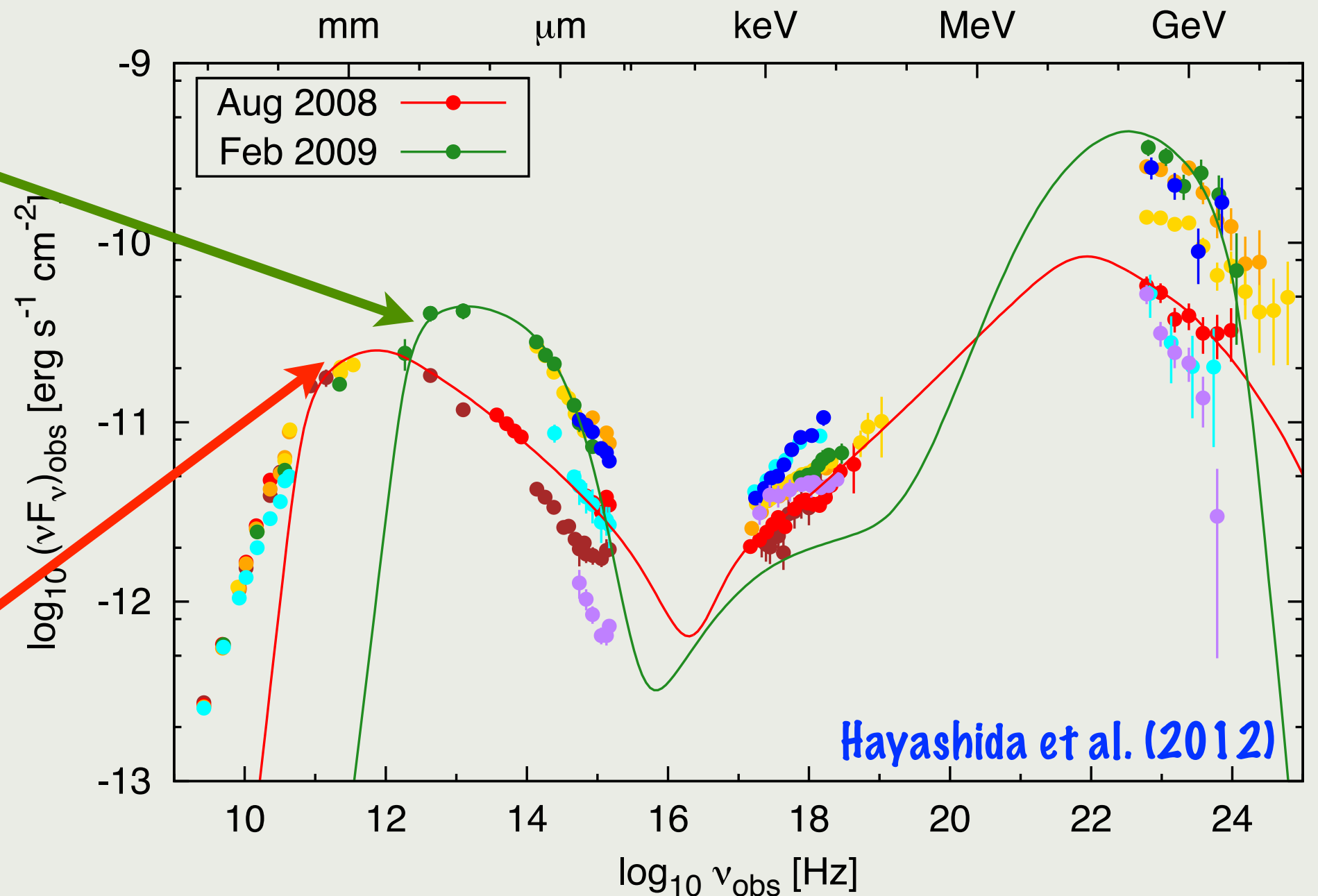


MAGNETIC FIELD STRENGTH FROM SYNCHROTRON SELF-ABSORPTION

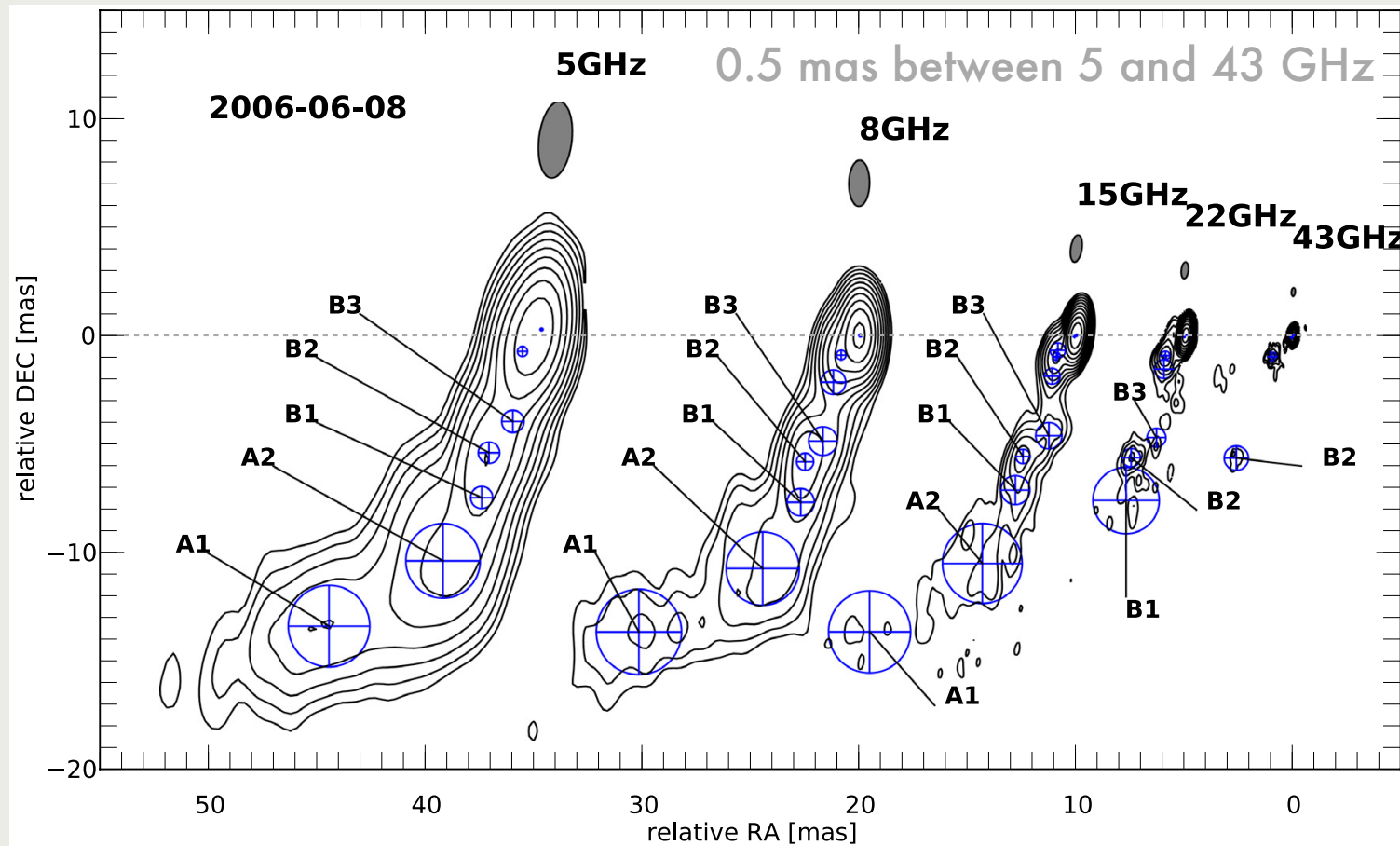
- $$\nu'_{SSA} \approx \frac{1}{3} \left(\frac{eB'}{m_e^3 c} \right)^{1/7} \frac{L'_{syn}{}^{2/7}}{R^{4/7}} \quad (\text{KN et al. 2014})$$

$R = 0.002 \text{ pc}$
 $r = 0.05 \text{ pc}$
 (BLR)

$R = 0.2 \text{ pc}$
 $r = 4 \text{ pc}$
 (HDR)



RADIO CORE SHIFTS



CTA 102; Fromm et al. (2013)

- $\Delta \propto \nu^{-1}$ for a conical jet

- $B' \propto \Delta^{3/4}$

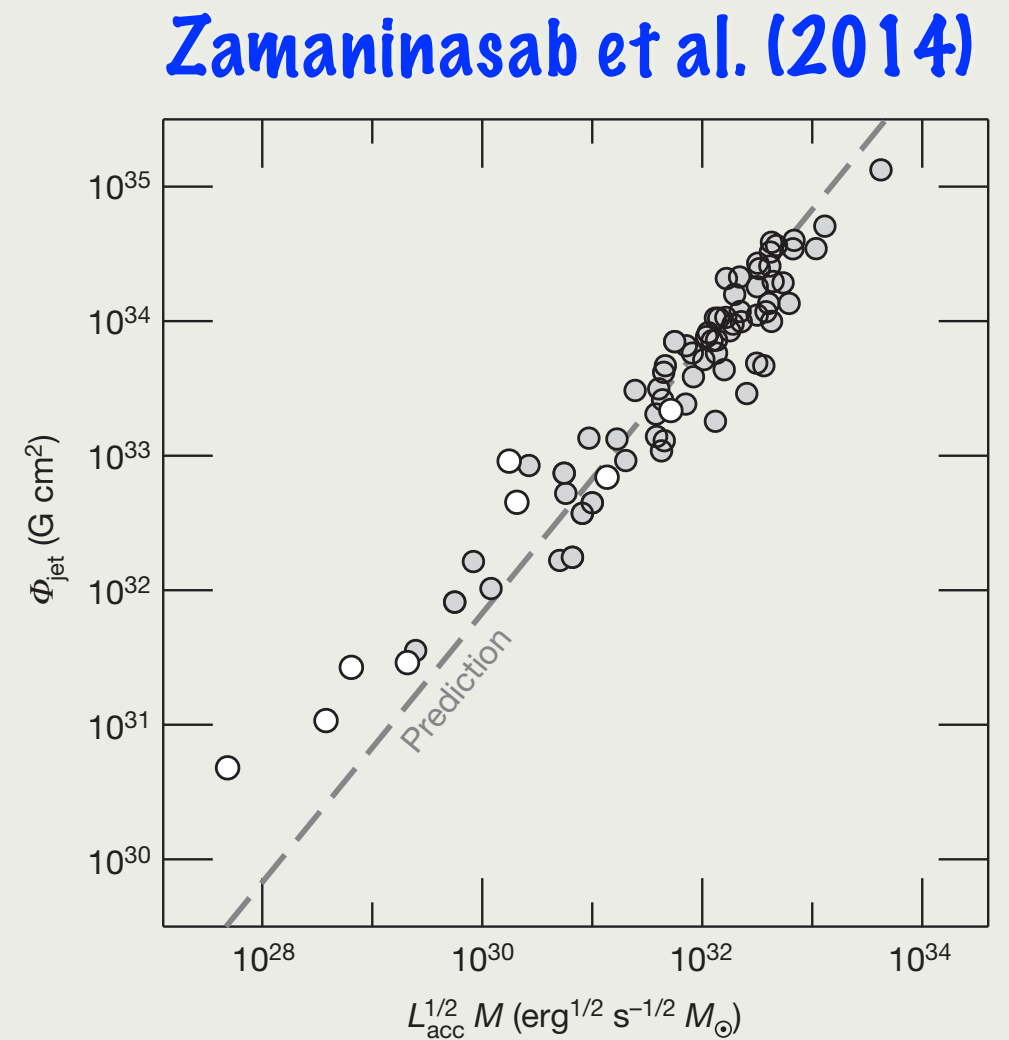


Figure 2 | Measured magnetic flux of the jet, Φ_{jet} , versus $L_{\text{acc}}^{1/2} M$. Here we assume that $\Gamma\theta_j = 1$; we also assume an accretion radiative efficiency of $\eta = 0.4$ for our sample of 76 sources. The dashed line shows the theoretical prediction based on the magnetically arrested disk model. Filled and open circles represent blazars and radio galaxies, respectively (see Methods for details).

FORMATION OF JETS

ROTATING MAGNETOSPHERE

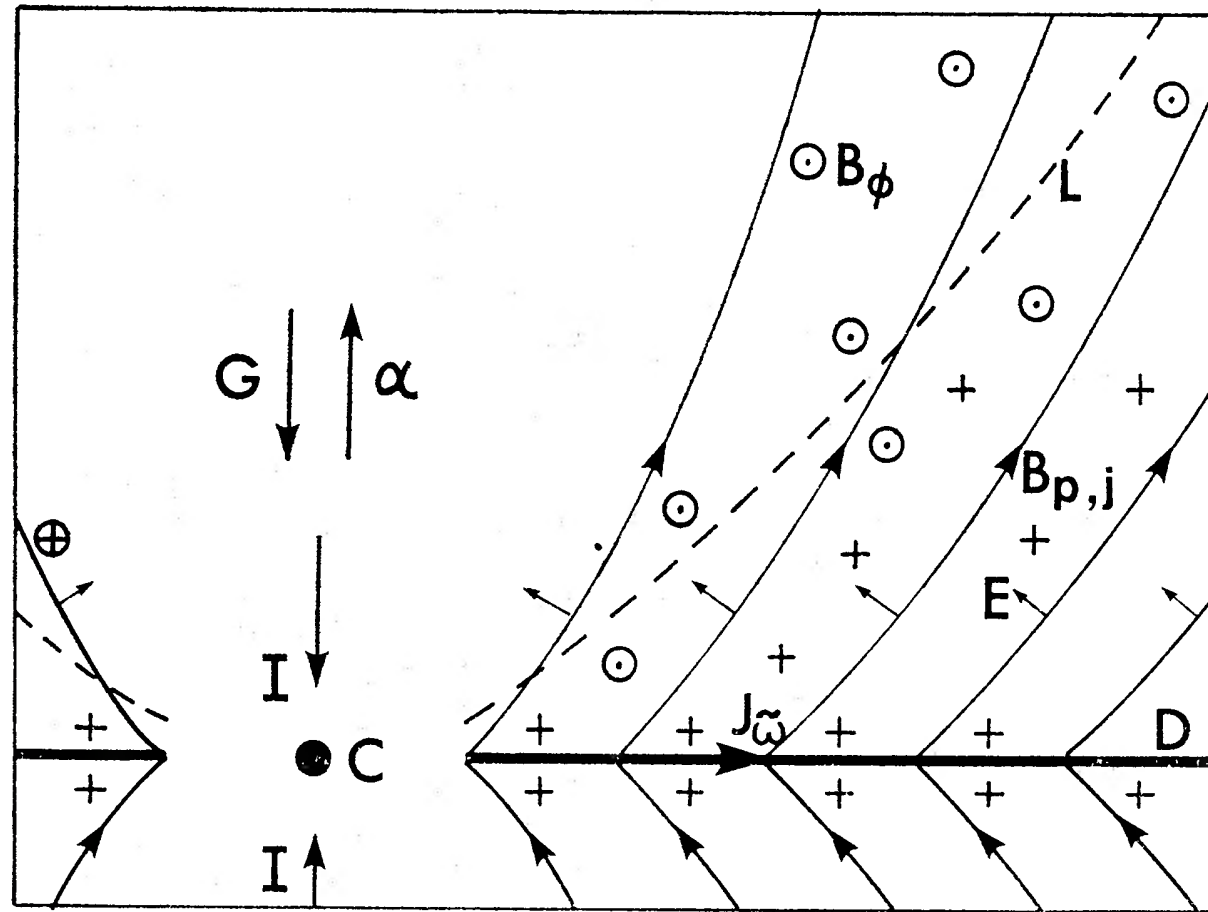


FIG. 1. Schematic representation of the magnetosphere above and below a magnetized accretion disc, D , surrounding a compact object, C . For the Newtonian solution (with $\alpha \cdot \mathbf{B} > 0$) described by equations (3.29)–(3.36), the poloidal field, B_p , lies on paraboloidal surfaces with the toroidal component, B_ϕ , becoming increasingly important as the light surface, L , is reached. The light surface drawn is appropriate for a Keplerian disc, $\alpha^2 = R_s c^2 / (2 \tilde{\omega}_0^3)$ where R_s is the Schwarzschild radius of the compact object. The current, j , and charge density, ρ , are related by $j \sim 2^{1/2} \rho c$ close to the disc.

Blandford (1976)

- Consider a magnetosphere with **poloidal fields** rooted in a rotating object (accretion disk).
- Rotating magnetosphere induces **perpendicular electric fields**.
- In the presence of plasma, **electric currents** will flow, redistributing electric charge.
- The currents induce **toroidal magnetic field** that produces an **outwards poloidal Poynting flux**.
- A stationary force-free solution can be calculated.

see also Lovelace (1976), Blandford & Payne (1982)

BLANDFORD-ZNAJEK (1977)

- Spinning (Kerr) black hole (BH) threaded by net magnetic flux.

- Power extracted from the BH:

$$P_{\text{BZ}} \propto \frac{a^2}{M_{\text{BH}}^2} \Phi_{\text{BH}}^2 \quad (\text{valid for } a \lesssim 0.3),$$

where a is the BH spin parameter, Φ_{BH} is the magnetic flux threading the BH horizon.

numerical demonstration:
Parfrey et al. (2019)

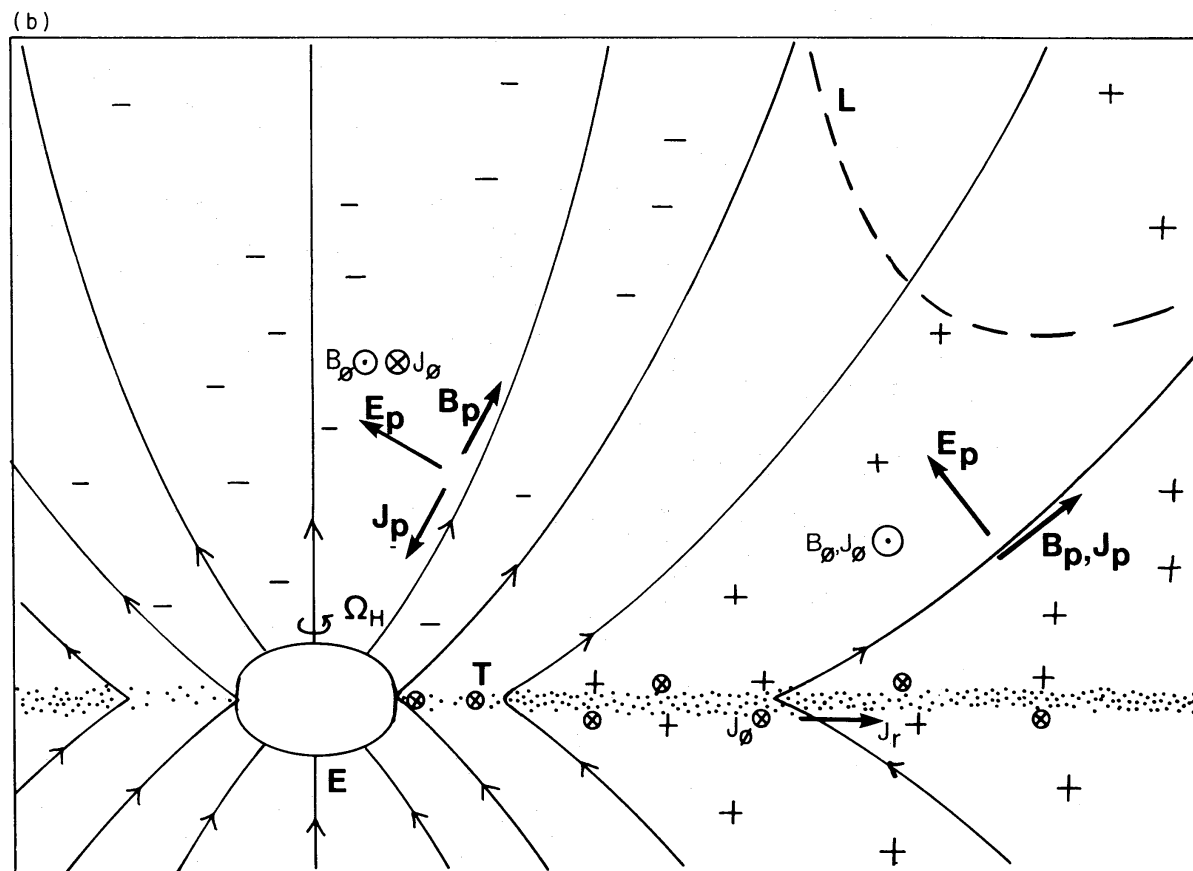
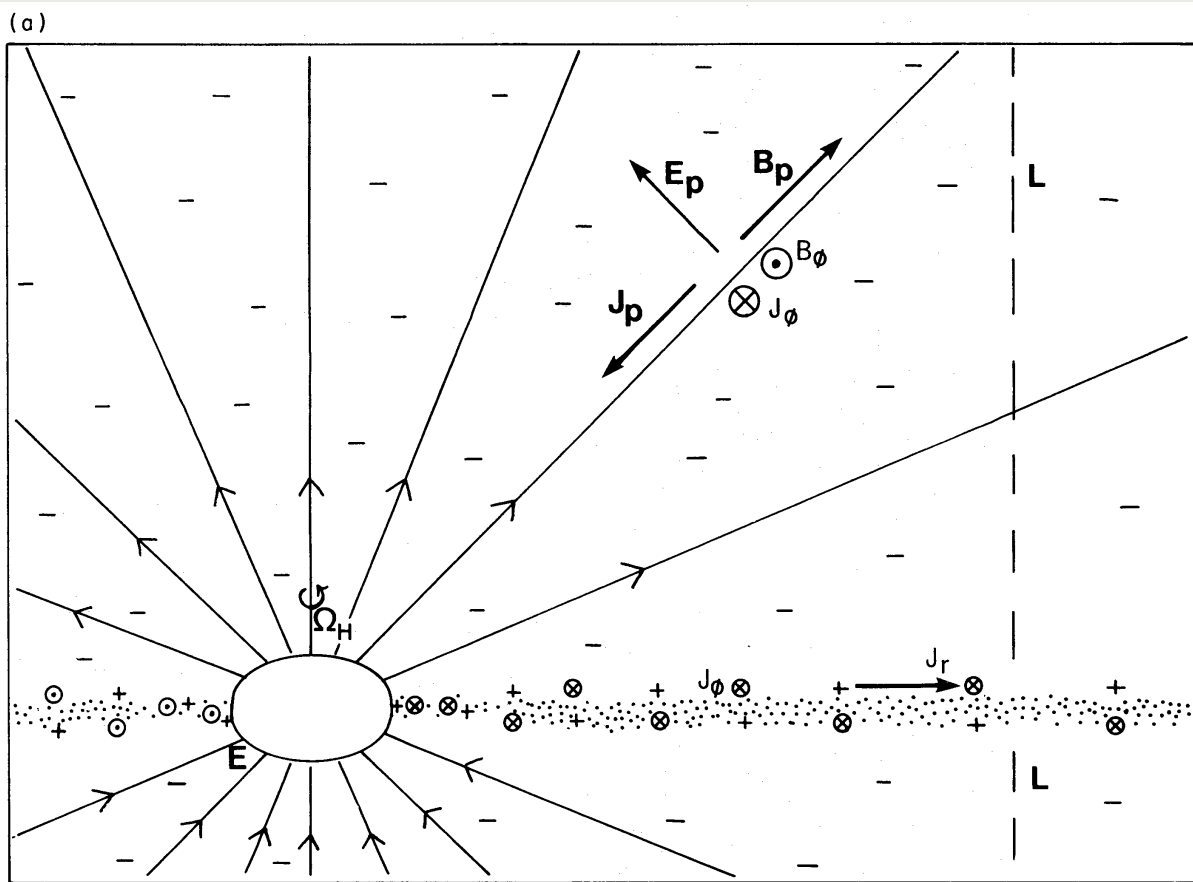


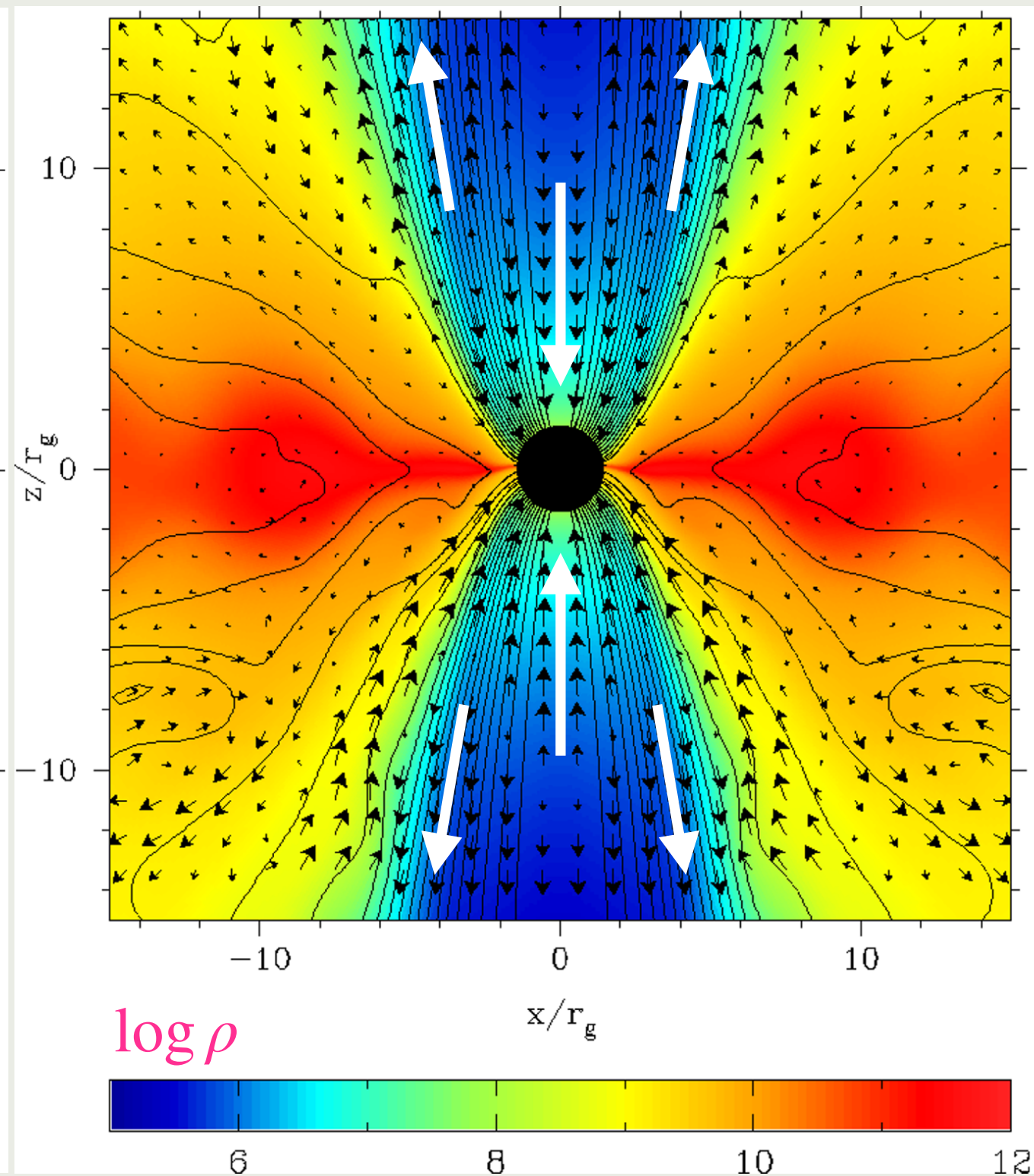
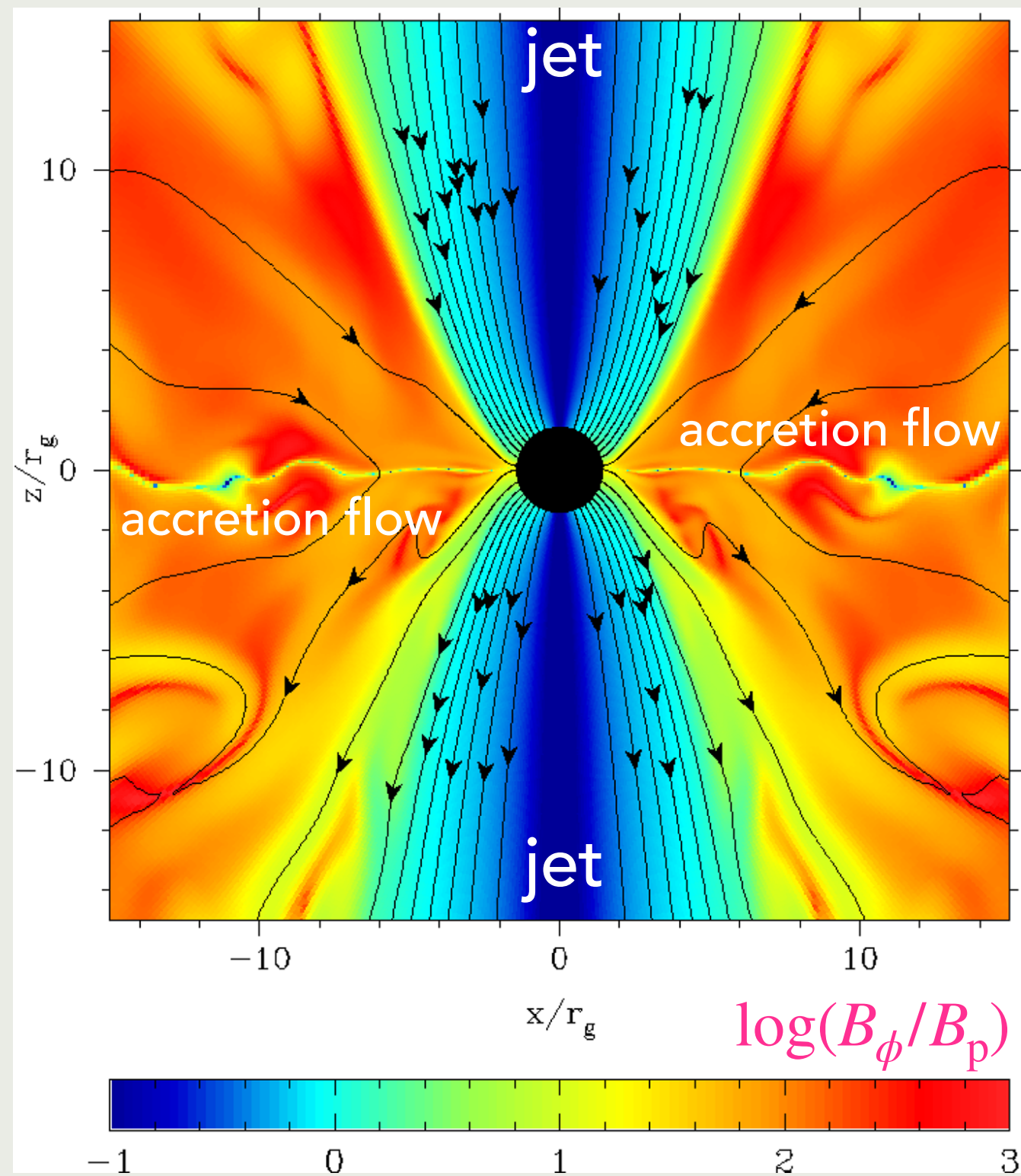
Figure 2. Electromagnetic structure of force-free magnetosphere with (a) radial and (b) paraboloidal magnetic fields. $\Omega_{\text{H}} \cdot \mathbf{B}$ is taken to be positive. Space charge, currents and non-zero field components shown are as seen by a static observer outside the ergosphere E. Physical observers travelling round the hole at constant r and θ and angular velocity $d\phi/dt$ will see the electric field reverse direction on the surface $d\phi/dt = \omega$. Inside this surface they see a Poynting flux of energy going towards the hole. (For a system of observers with time-like worldlines $d\phi/dt \rightarrow \Omega_{\text{H}}$ on the event horizon and $d\phi/dt \rightarrow 0$ at infinity. Hence when $0 < \omega < \Omega_{\text{H}}$, i.e. when the hole is losing energy electromagnetically, this surface always exists.) The discs are assumed to be Keplerian; the electromagnetic structure of the magnetosphere of the transition region, T, in (b) cannot be determined without additional assumptions. Outside this region Blandford's (1976) Newtonian solution applies. Note the difference in the shape of the light surface, L, in the two cases. For a paraboloidal field the energy appears to be focussed along the rotation axis.

PROBLEM 8: BLACK HOLE FIELD

- Estimate (order of magnitude) the magnetic field strength in the immediate vicinity of a black hole of mass (1) $10M_{\odot}$, (2) 10^9M_{\odot} sufficient to drive a Poynting flux (through the $4\pi R_{\text{Sch}}^2$ cross section) equal to the Eddington luminosity.

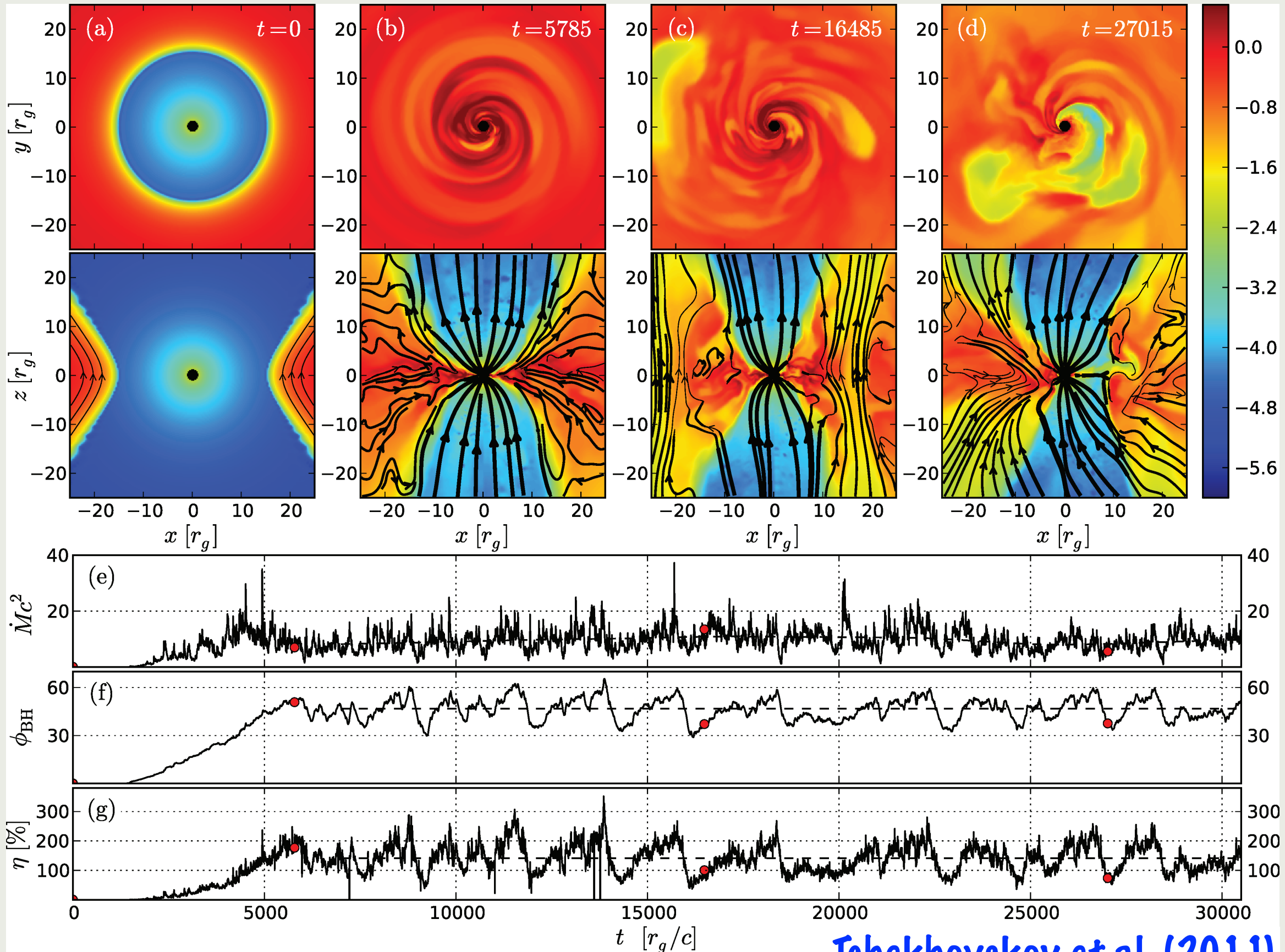
This problem is worth 5 points. Solutions should be sent as 1-page PDF files to knalew@camk.edu.pl before the next lecture.

LAUNCHING RELATIVISTIC JETS FROM ACCRETING BLACK HOLES



Barkov & Komissarov (2008)

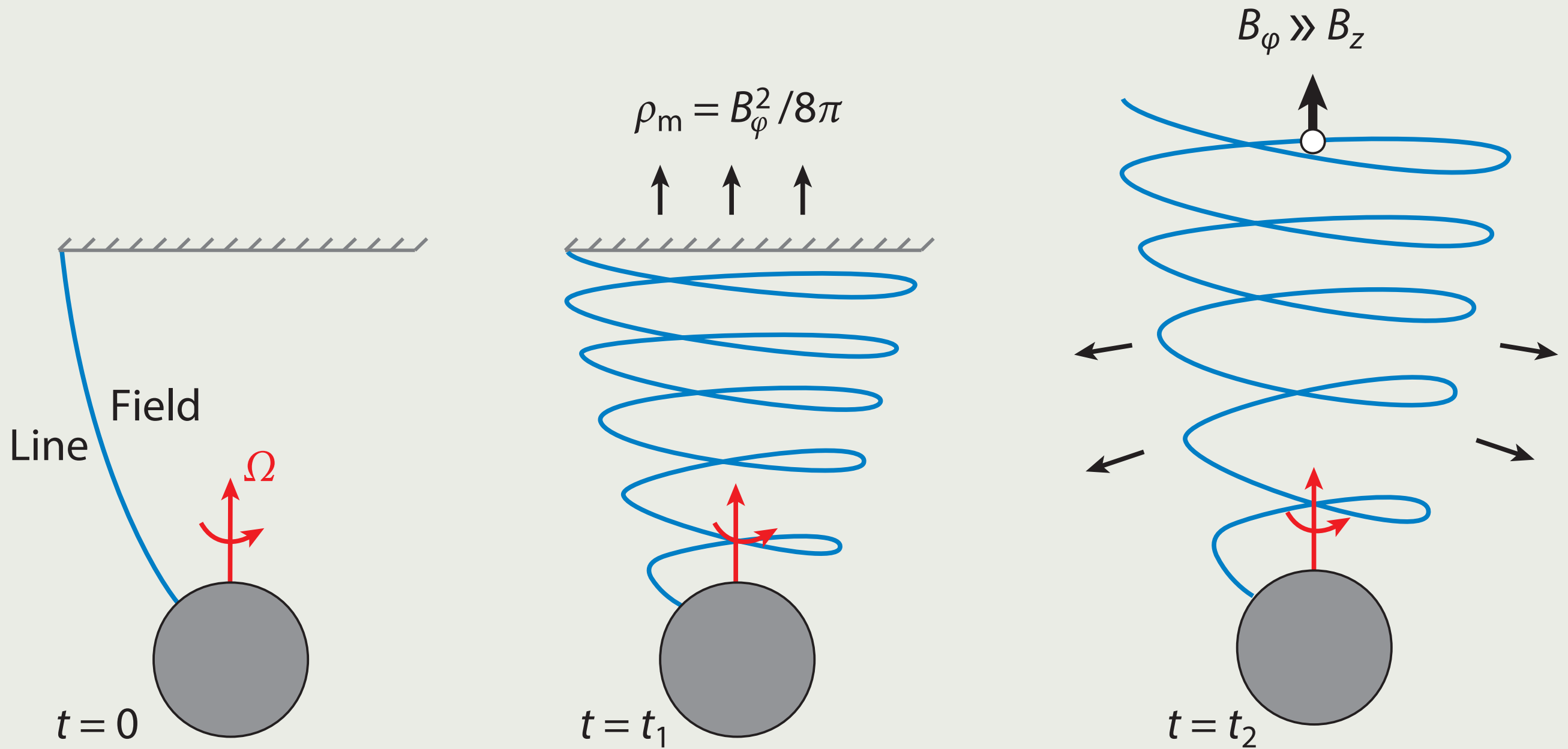
MAXIMUM JET POWER



$$\eta \simeq \frac{P_j}{\dot{M}c^2}$$

Tchekhovskoy et al. (2011)

ACCELERATION OF JETS



ACCELERATION OF JETS

- Conservation of energy for perpendicular co-moving magnetic field $\vec{B}' \perp \vec{v}$:

$$T^{0i} = \Gamma^2 \left(w' + \frac{B'^2}{4\pi} \right) \frac{v^i}{c} = \Gamma^2 (1 + \sigma') w' \beta^i = \text{const},$$

where $\sigma' = \frac{B'^2}{4\pi w'}$ is the magnetization

- Conservation of mass:

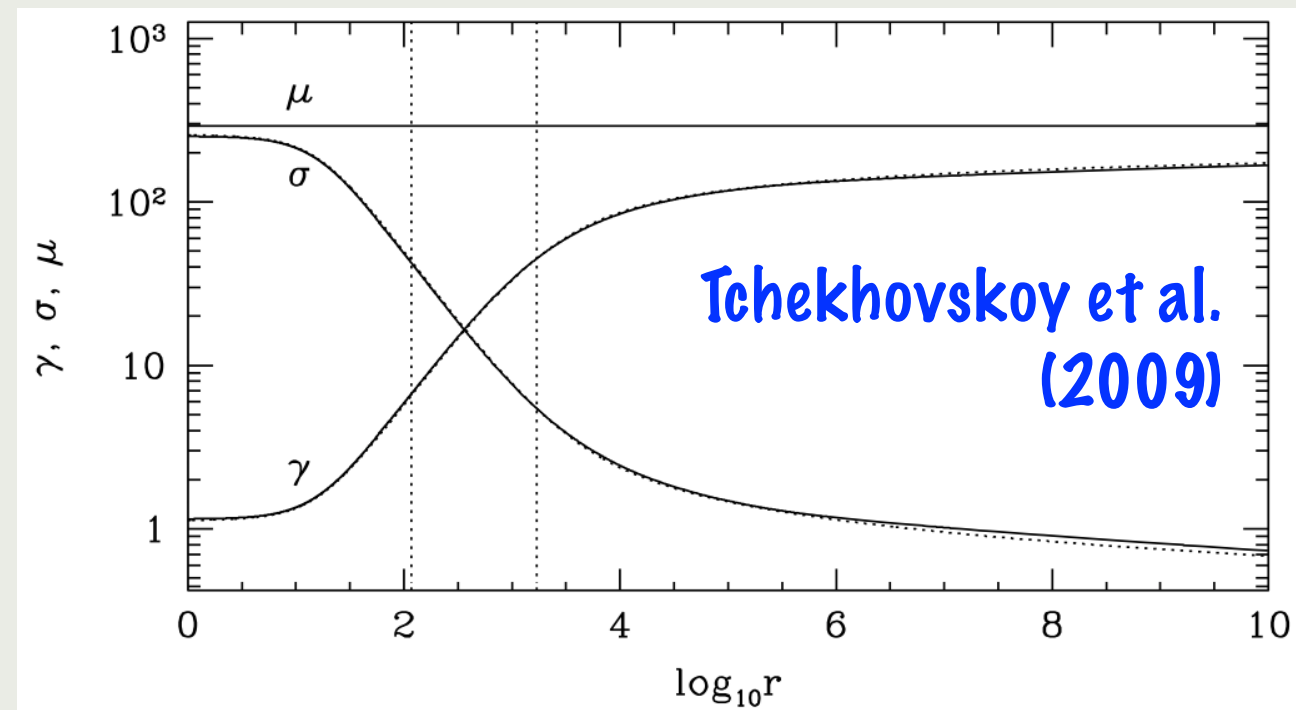
$$\Gamma \rho' \beta^i = \text{const}$$

- Bernoulli's equation:

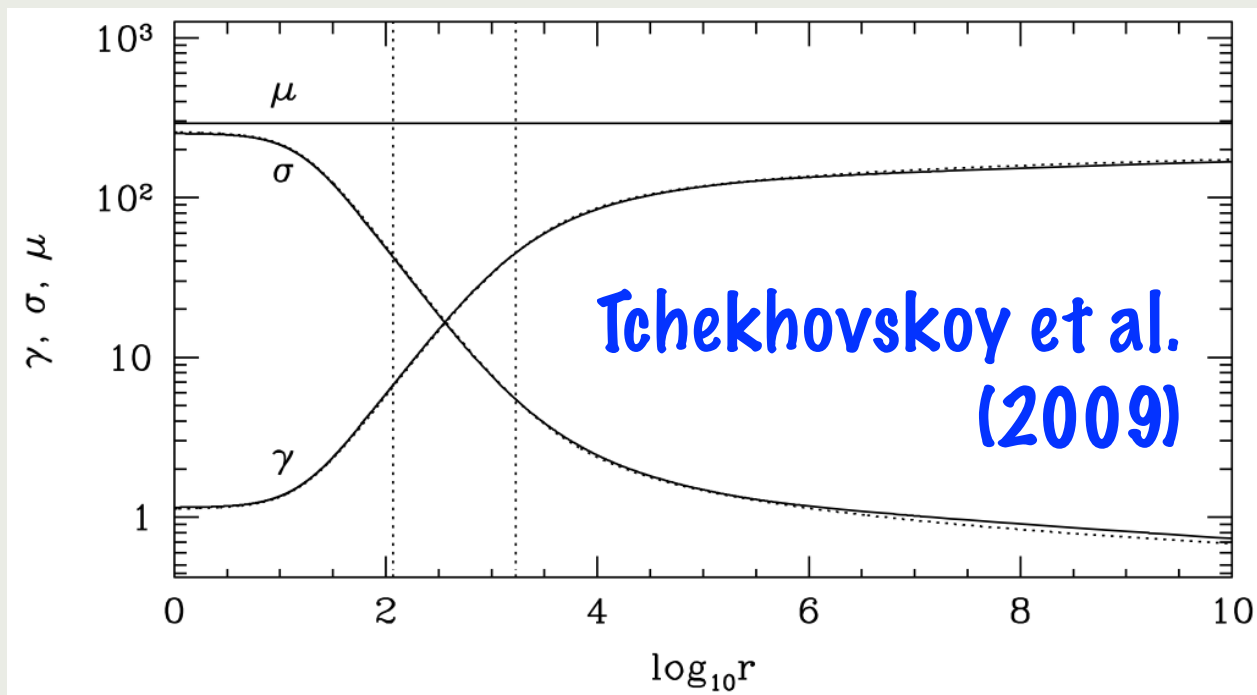
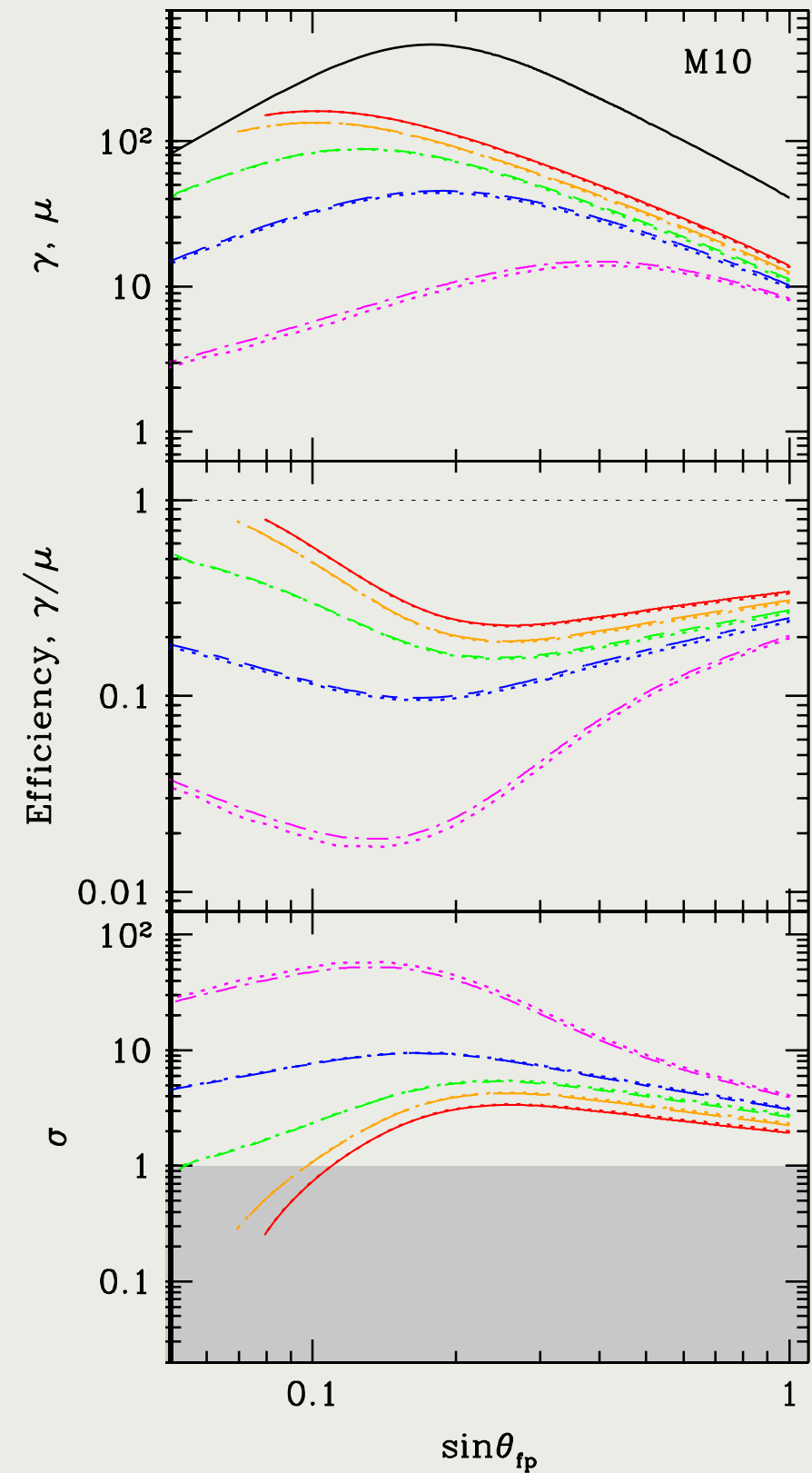
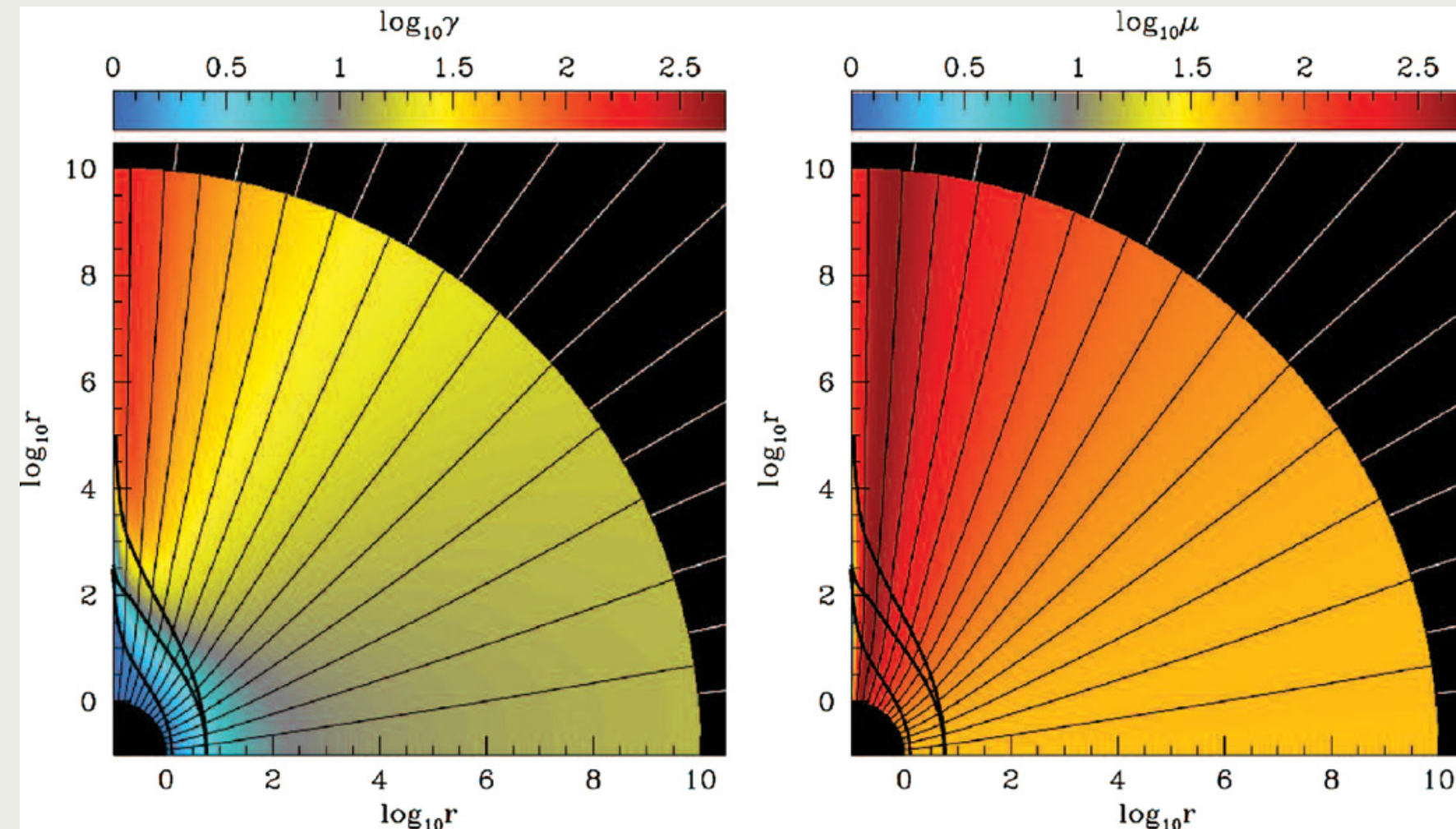
$$\frac{T^{0i}}{\Gamma \rho' \beta^i} = \Gamma (1 + \sigma') \frac{w'}{\rho'} \equiv \mu \frac{w'}{\rho'} = \text{const},$$

where $\mu \equiv \Gamma(1 + \sigma')$ is the Michel parameter

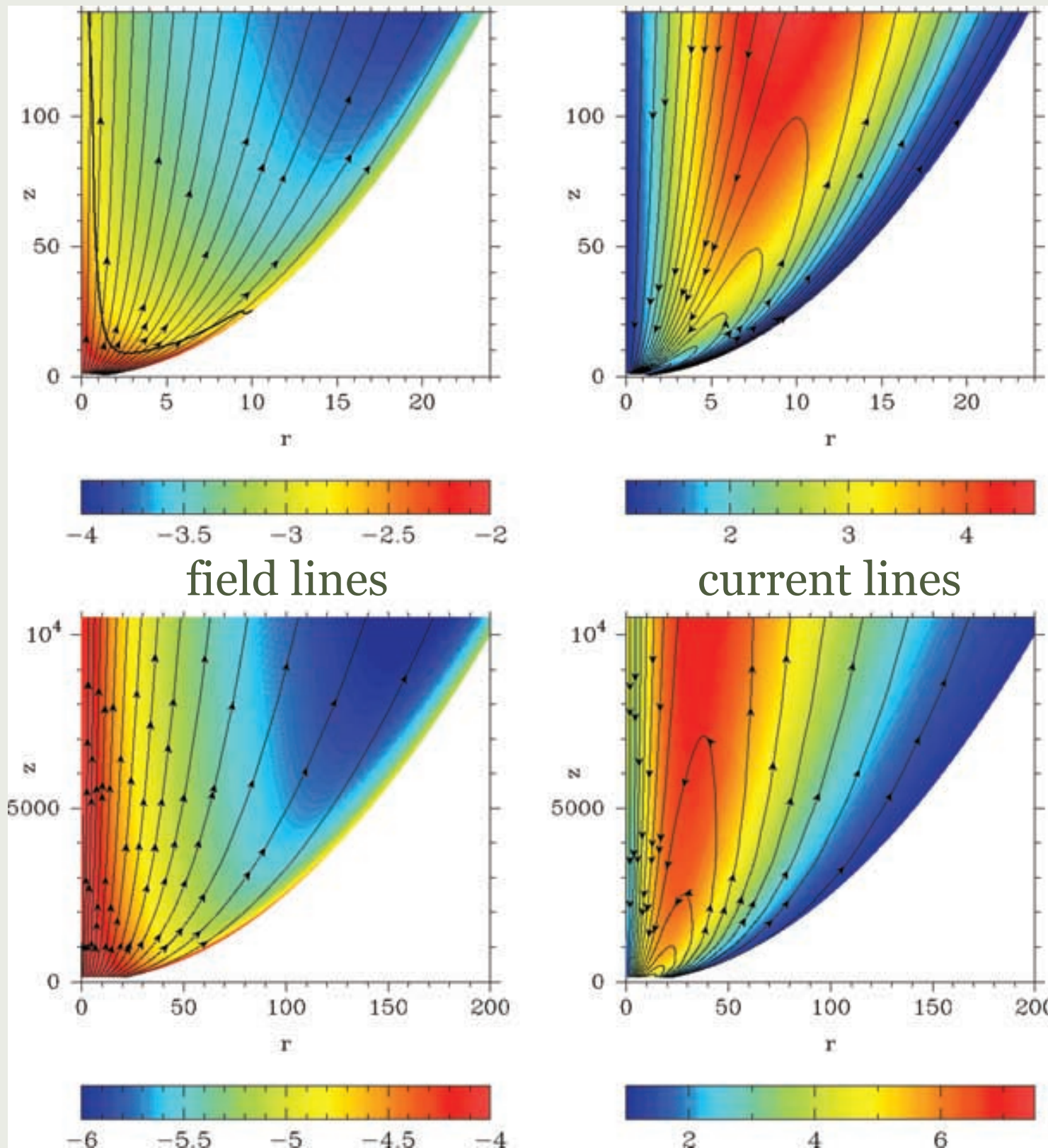
- Conservation of momentum: $T^{ij} = \text{const}$



ACCELERATION OF JETS RADIAL FIELD (SPLIT MONOPOLE)



ACCELERATION OF JETS PARABOLOIDAL FIELD (COLLIMATION)

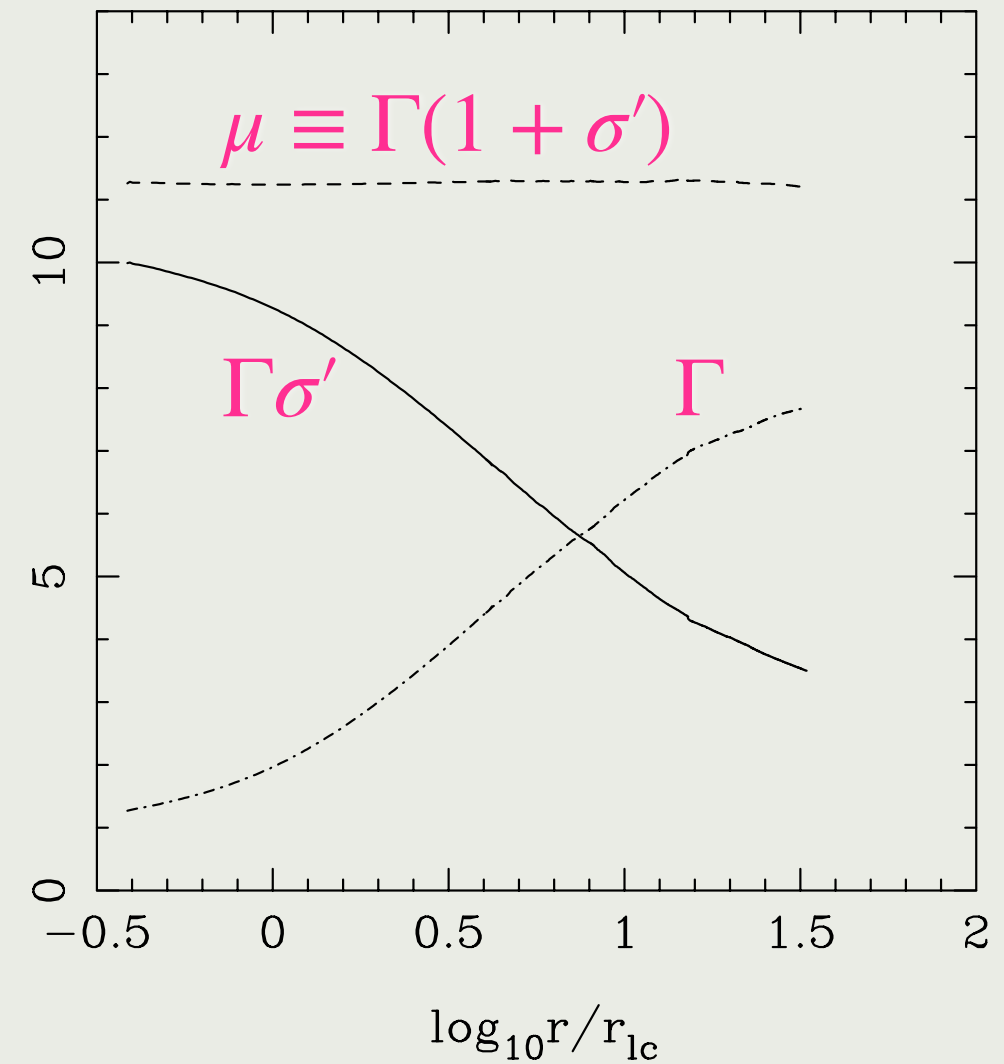


field lines

current lines

$\log(\Gamma\rho')$

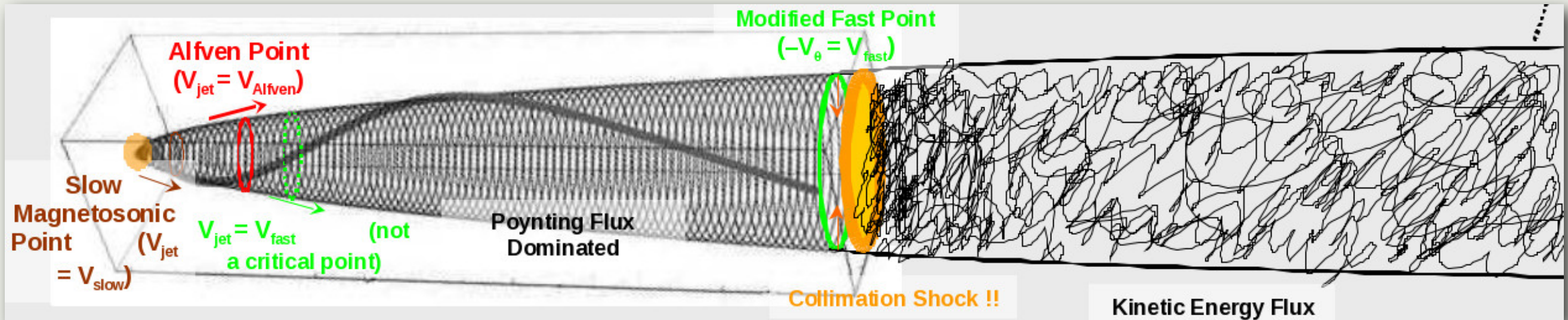
Γ



Komissarov et al. (2007)

BEYOND MAGNETICALLY DOMINATED JETS

D. Meier



acceleration-collimation zone

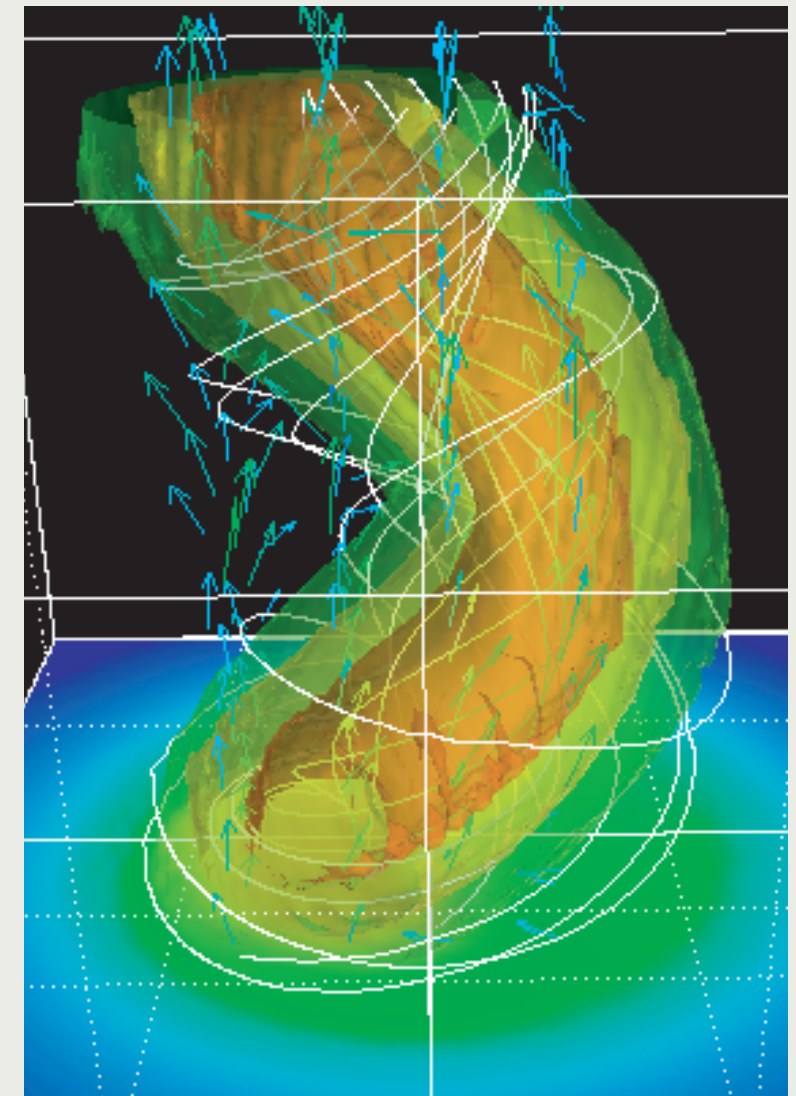
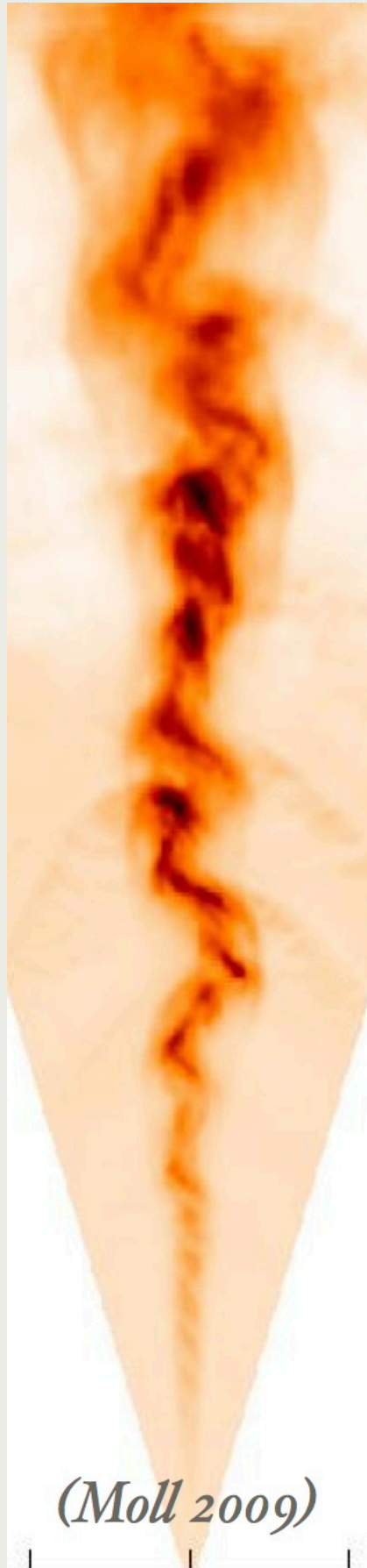
dissipation (blazar) zone

- As the jets become relativistically fast, they convert from being dominated by magnetic energy (Poynting flux) to being dominated by kinetic energy (inertia).
- As the magnetic fields become weak, they may be subject to instabilities disrupting the ordered structure and leading to turbulent motions, making the fields chaotic.
- Dissipation of ordered energy (kinetic by shocks, magnetic by reconnection) leads to non-thermal particle acceleration and blazar emission.

INSTABILITIES IN MAGNETIZED JETS

INSTABILITIES OF JETS WITH TOROIDAL MAGNETIC FIELDS

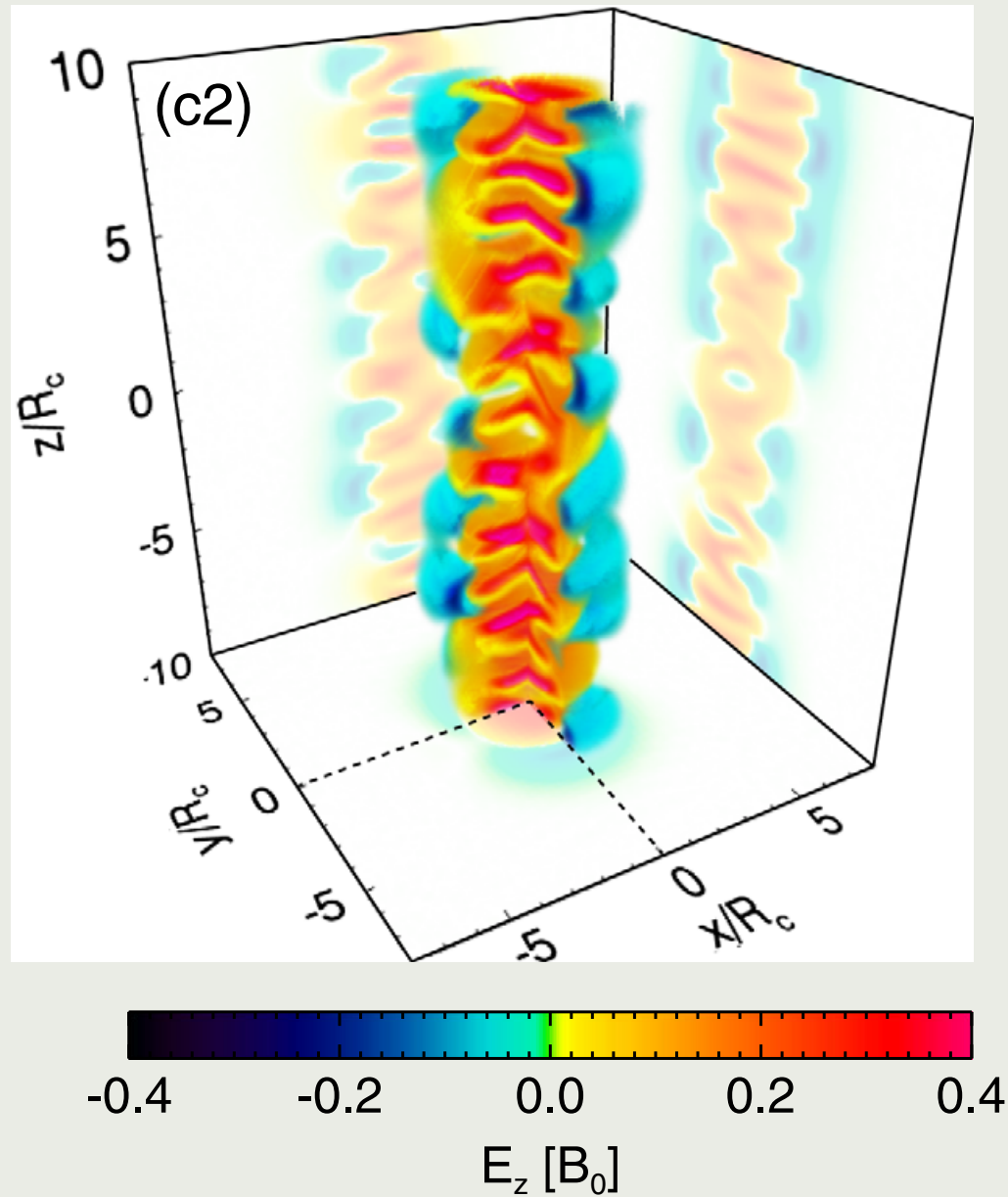
- toroidal magnetic field supported by gas pressure is unstable
(Kruskal & Schwarzschild 1954)
- magnetic fields in expanding jets become increasingly toroidal
 $B_{\phi} \propto R^{-1}$, $B_p \propto R^{-2}$
- jets may need to dissipate their magnetic fields via magnetic reconnection
(Giannios & Spruit 2006)



Mizuno et al. (2011)

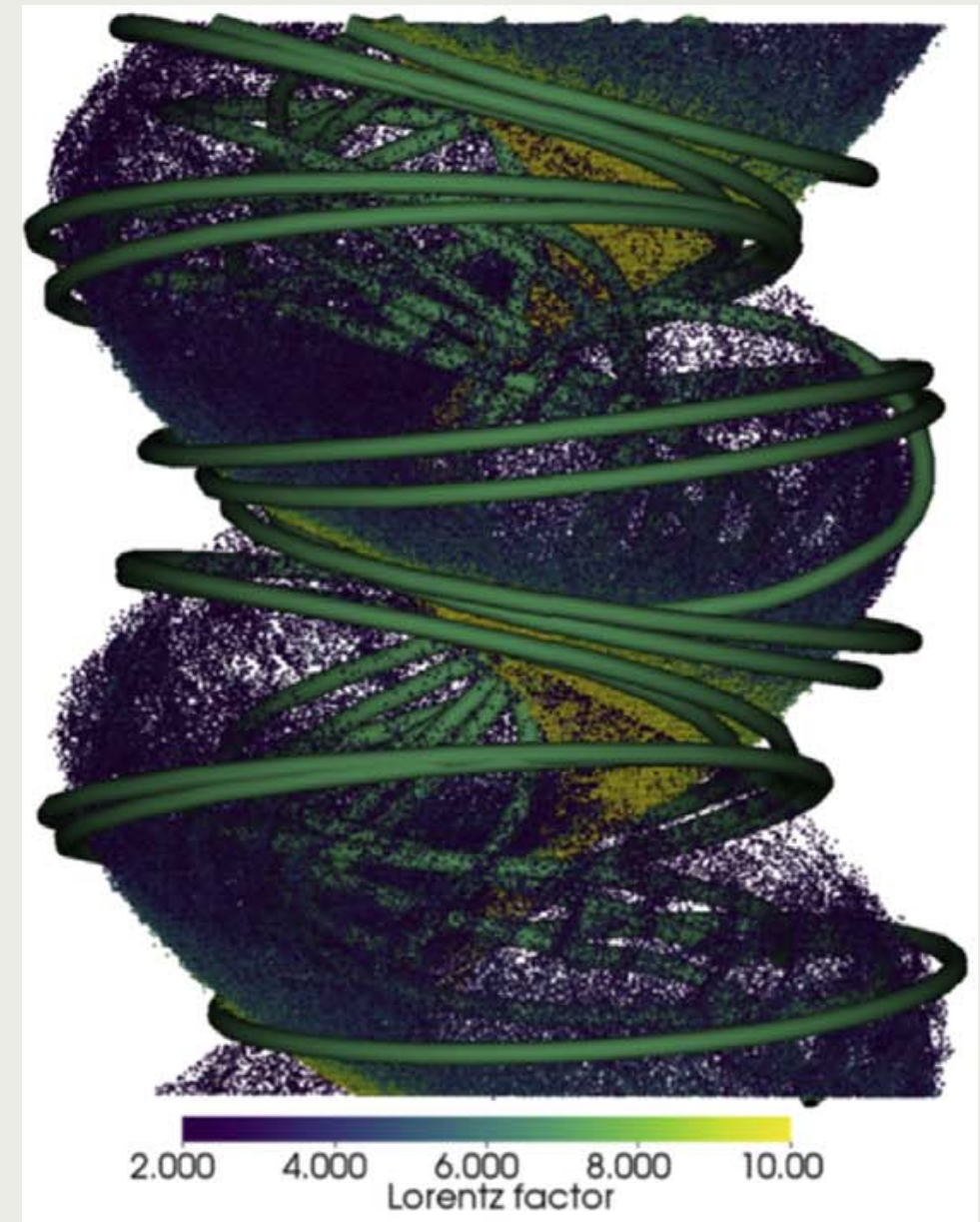
KINETIC SIMULATIONS OF INSTABILITIES IN CYLINDRICAL JETS WITH TOROIDAL MAGNETIC FIELDS

gas pressure balanced
(Z-pinch)



Alves, Zrake & Fiuza (2018)

axial magnetic field balanced
(force-free screw-pinch)

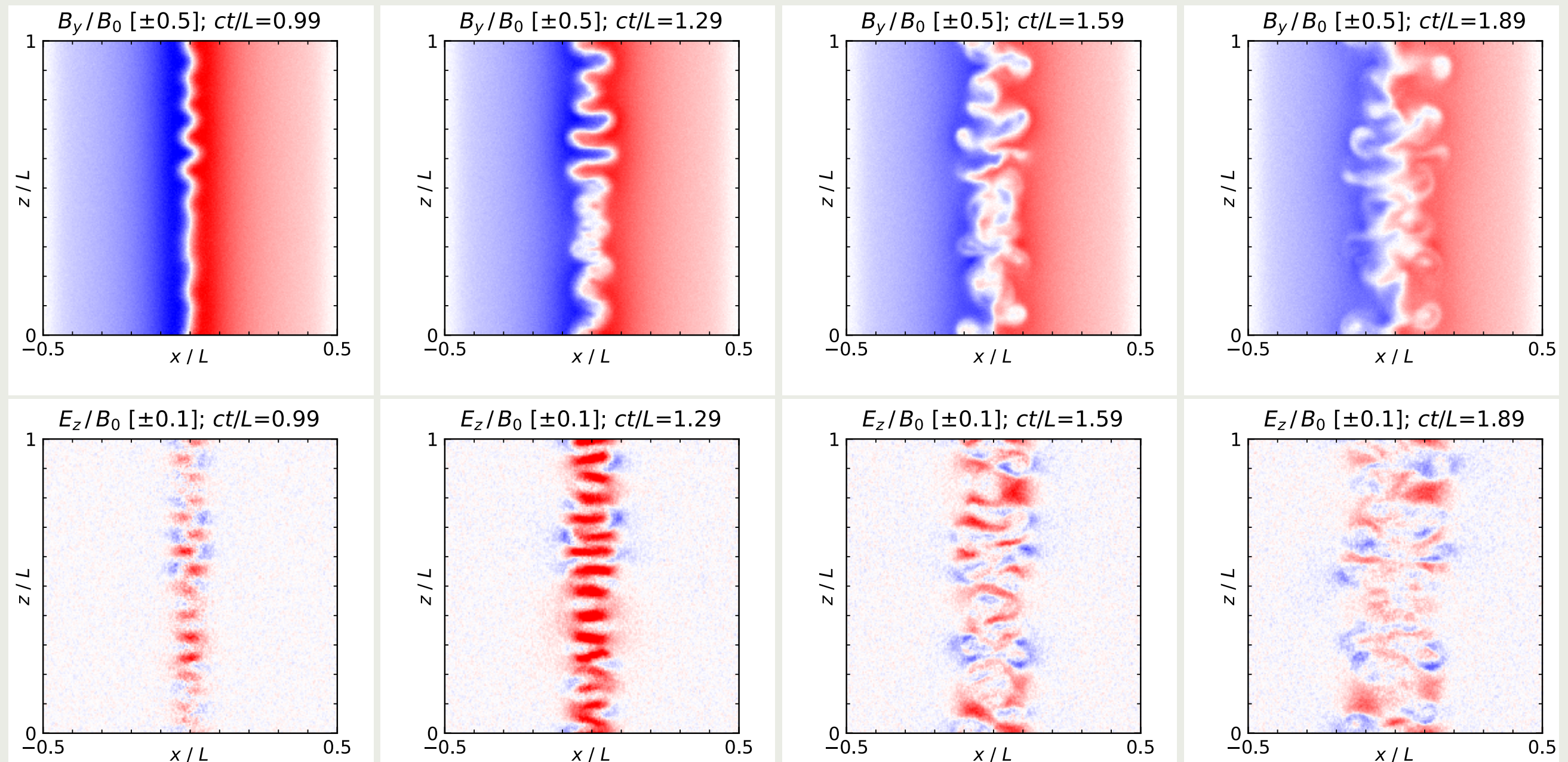


Davelaar, Philippov, Bromberg & Singh (2020)

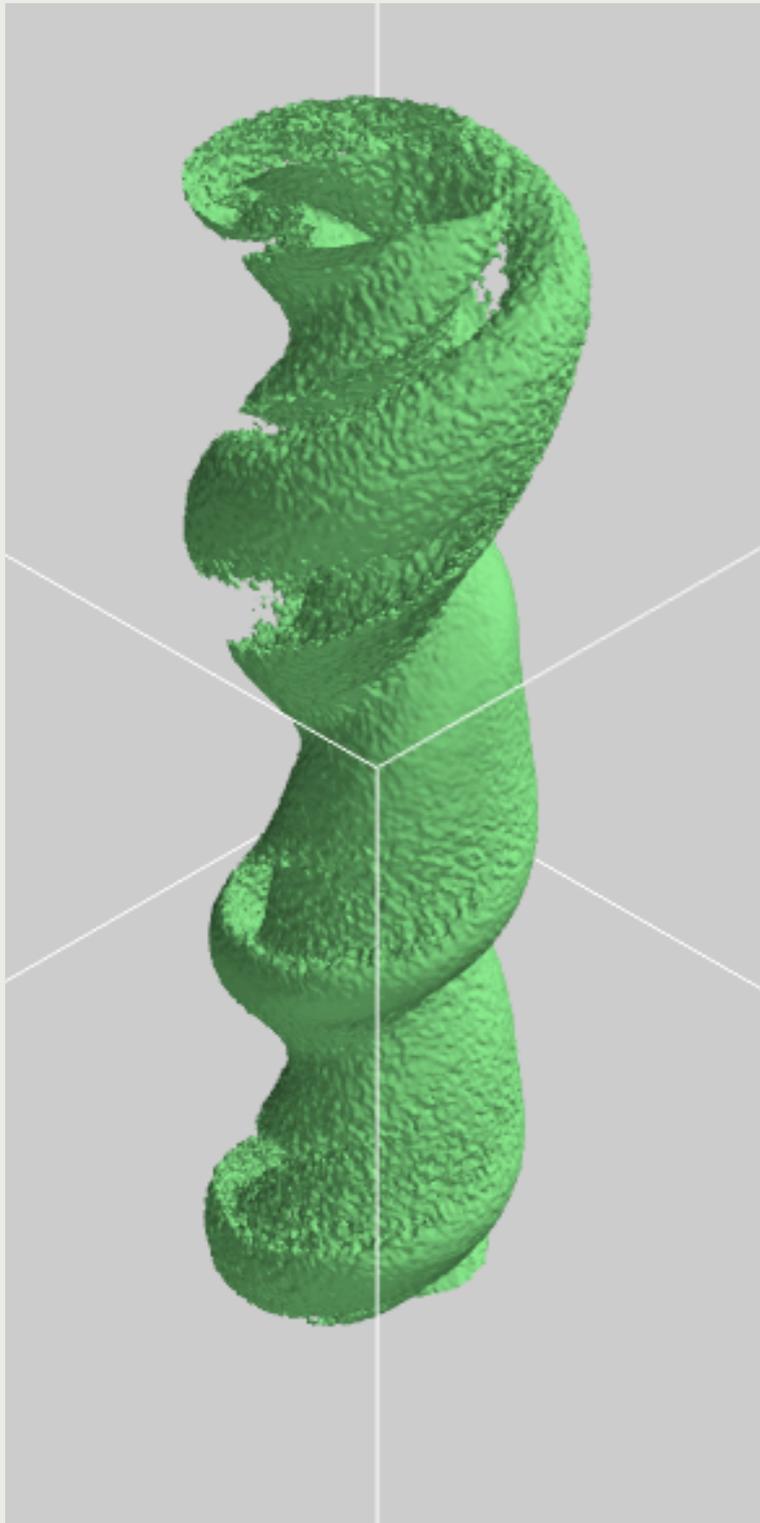
efficient particle acceleration found in both cases

KINETIC SIMULATIONS OF INSTABILITIES IN CYLINDRICAL JETS WITH TOROIDAL MAGNETIC FIELDS

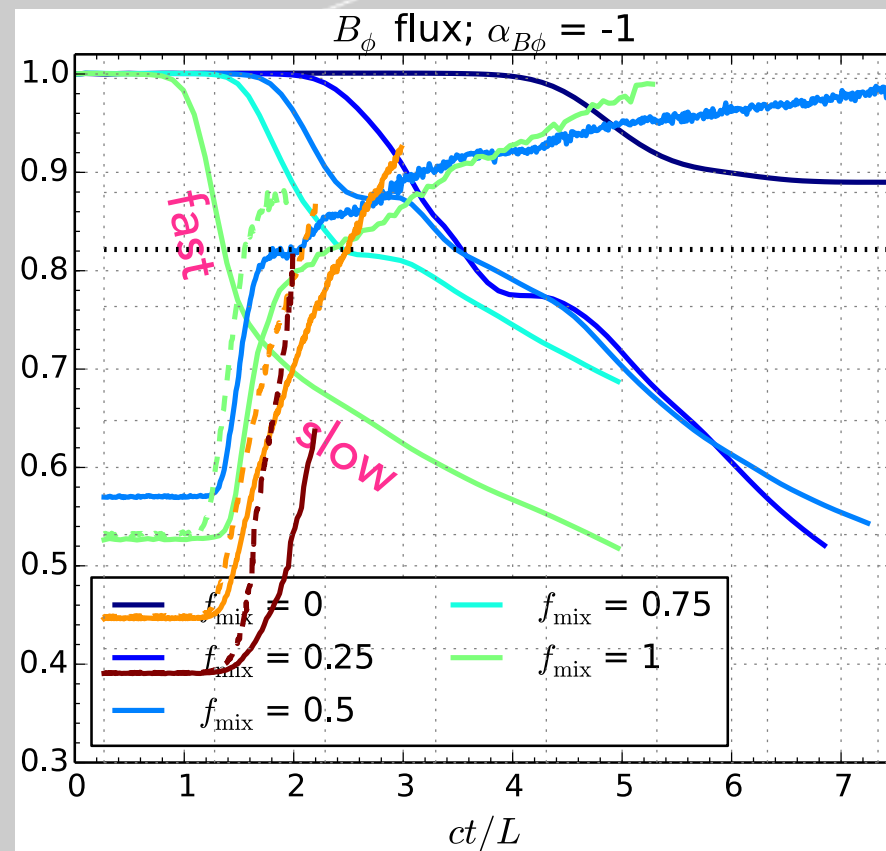
3D, periodic boundaries, static equilibrium, pair plasma
moderately relativistic magnetization, highly relativistic temperature



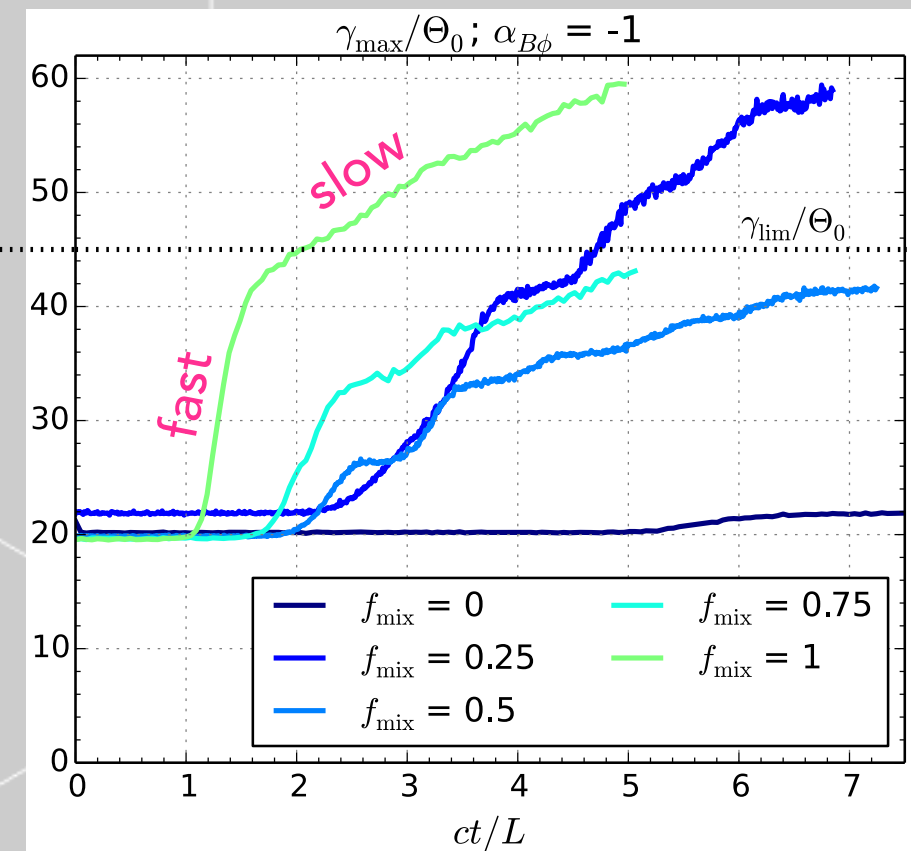
KINETIC SIMULATIONS OF INSTABILITIES IN CYLINDRICAL JETS WITH TOROIDAL MAGNETIC FIELDS



B_ϕ flux dissipation



particle acceleration



- fast magnetic dissipation and particle acceleration by $\vec{E} \perp \vec{B}$ until the confinement limit $\gamma_{\text{lim}} = eB_0R_0/mc^2$ (Alves et al. 2018)

SUMMARY

- Jets are collimated outflows from certain accreting black holes characterized by highly relativistic speeds appearing as superluminal.
- Radiation from a relativistic jet viewed at a small angle is very strongly boosted (Doppler effect + aberration).
- Jets are powered by Poynting flux induced in a rotating magnetosphere with poloidal and toroidal fields.
- Acceleration of jets to relativistic speeds involves conversion of relativistic magnetization aided by collimation.